Combined UV-Temperature-Humidity Accelerated Testing of PV Modules:

Reliability of UV-cut and UV-pass EVA Encapsulants

by

Pooja Arularasu

A Thesis Presented in Partial Fulfillment
of the Requirements for the Degree
Master of Science

Approved April 2019 by the
Graduate Supervisory Committee:

Govindasamy Tamizhmani, Co-Chair
Bin Mu, Co-Chair
Arul Mozhy Varman

ARIZONA STATE UNIVERSITY

May 2019

ABSTRACT

In the past, the photovoltaic (PV) modules were typically constructed with glass superstrate containing cerium oxide and EVA (ethylene vinyl acetate) encapsulant containing UV absorbing additives. However, in the current industry, the PV modules are generally constructed without cerium oxide in the glass and UV absorbing additives in EVA to increase quantum efficiency of crystalline silicon solar cells in the UV regions. This new approach is expected to boost the initial power output of the modules and reduce the long-term encapsulant browning issues. However, this new approach could lead to other durability and reliability issues such as delamination of encapsulant by damaging interfacial bonds, destruction of antireflection coating on solar cells and even breakage of polymeric backbone of EVA. This work compares the durability and reliability issues of PV modules having glass without cerium oxide and EVA with (aka, UVcut or UVC) and without (aka, UVpass or UVP) UV absorbing additives. In addition, modules with UVP front and UVC back EVA have also been investigated (aka, UVhybrid or UVH). The mini-modules with nine split cells used in this work were fabricated at ASU's Photovoltaic Reliability Laboratory. The durability and reliability caused by three stress variables have been investigated and the three variables are temperature, humidity/oxygen and UV dosage. The influence of up to 800 kWh/m^2 UV dosage has been investigated at various dosage levels. Many material and device characterizations have been performed to ascertain the degradation modes and effects. The UVC modules showed encapsulant discoloration at the cell centers as expected but the UVH modules showed a ring-shaped encapsulant discoloration close to the cell edges as evidenced in the UV fluorescence (UVF) imaging study. The PV modules containing

UVP on both sides of cells with limited access to humidity or oxygen through backsheet (covered backsheet with adhesive aluminum tape) seem to experience encapsulant delamination as evidenced in the UVF images. Plausible explanations for these observations have been presented.

To,

My father, mother, and my lovely sister for their boundless love and forever support

ACKNOWLEDGMENTS

TABLE OF CONTENTS

LIST OF TABLES

LIST OF FIGURES

1   INTRODUCTION

1.1   **Background**

A renewable and clean energy supply, solar energy can meet the global energy demands for an extended period. They operate by the absorption of photons from sunlight, generate electron-hole pairs, and convert them to electricity. Though the weather conditions like temperature, humidity deteriorate the performance of PV and bring down its power, the impact of weather condition on the generation of solar energy has not been given importance because the research mainly focuses on improving the efficiency of the PV modules by the application of new materials that provide increased efficiency [1].

A typical crystalline silicon PV module is of Glass-Encapsulant-Solar cell-Encapsulant-Back sheet construction. A significant number of PV modules degrades and fails much earlier than their warranty period due to the problems (browning and delamination) in the encapsulant. For the proper operation of the PV module, the encapsulant should maintain good transmissivity throughout the module's lifetime so that the light reaches the solar cell. The encapsulant should support good adhesion module components and protect cell and metallization from external impacts. In terms of reliability of PV modules, properties of encapsulant are crucial in terms of UV irradiation, humidity, temperature cycles, extremely low or high ambient temperatures, mechanical loads, electric potential relative to ground, etc [2].

The encapsulant of the solar module gets affected by the irradiance. Because of its high energy, ultraviolet radiation is a stressful factor that causes polymer degradation in solar

cells. The photons present in the UV light activates the components in the polymer resulting in free radical production. As a result, oxidation and other reactions take place which degrades the polymer. Forencapsulant, different photothermal and thermal reactions can happen together with UV radiation from light. Norrish I and Norrish II are the main degradation reactions that take place in the EVA. The vinyl acetate group in the main chain forms acetaldehyde and certain other gases which lead to bubble formation in the PV module in the Norrish I reaction. In Norrish II formation of polyenes (C=C) takes place which is the major contributing factor for the discoloration of the EVA. In addition to this, there is acetic acid production which acts as a catalyst for the discoloration reactions [3]. *Figure 1.1 [4]* shows the main degradation agents of PV cells.
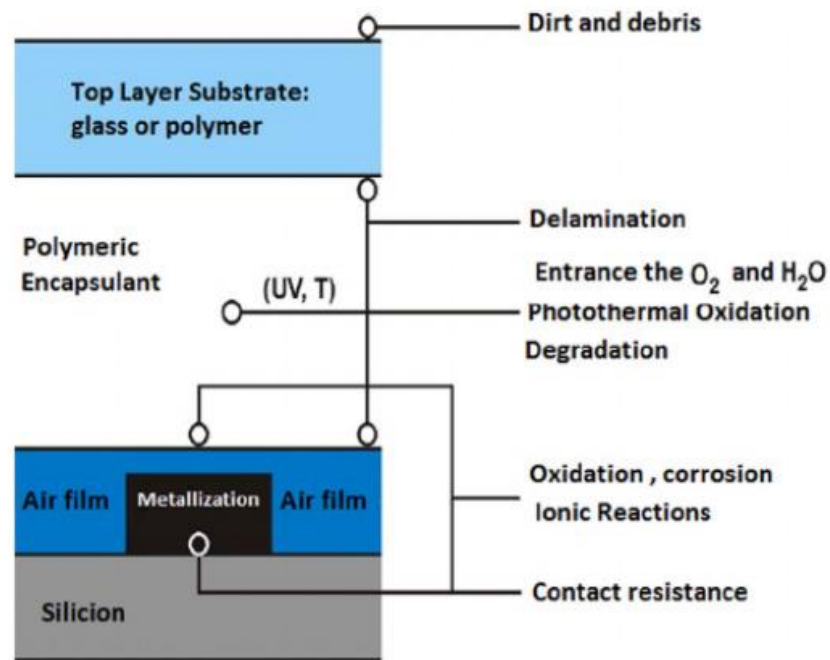
Figure 1.1: Main degradation agents and possible degradation mechanism in PV [4]

Light traveling through a medium gets reflected, transmitted, refracted or absorbed. In regions of high humidity, as per the facts when the light consisting of energy/photon strikes the denser water layer, refraction appears which results in decreasing of the intensity of the light which appears the root cause of the lowering of efficiency [5]. Humid places like Florida has a hot, humid climate. Humidity in the form of water layer gets settled on PV modules. The moisture reduces light transmission by incident light scattering. The hydrolysis of the copolymer also results in acidification or depolymerization [3].

In the presence of humidity, the cell degrades, and corrosion occurs at the leads and busbars. There will be moisture ingress through the backsheet under humid conditions. Degradation reaction also happens at the interfaces. Delamination occurs by the hydrolysis of the siloxane bond between the silane agent present between the glass and the encapsulant. Delamination promotes water ingression, reduced dissipation of heat. Under humid conditions corrosion also occurs at the leads and busbars. In areas of high humidity, there will be moisture permeation through the backsheet. Under humidity degradation mechanisms are noted at the interfaces. Delamination serves as a pathway for the ingression of water and results in reduced dissipation of heat [3].

Humidity may be absolute or relative. Absolute humidity is the amount of water vapor in a unit volume of air. It is expressed in kilograms per cubic meter. It does not change according to the temperature of the air. When there is a high amount of water vapor in the atmosphere, absolute humidity will also be high. Relative humidity is the percentage or ratio of the amount of water vapor in a volume of air at a given temperature and the amount that it can hold at that given temperature. The amount of water vapor in warm air will result in a lower relative humidity than in cold air [6].
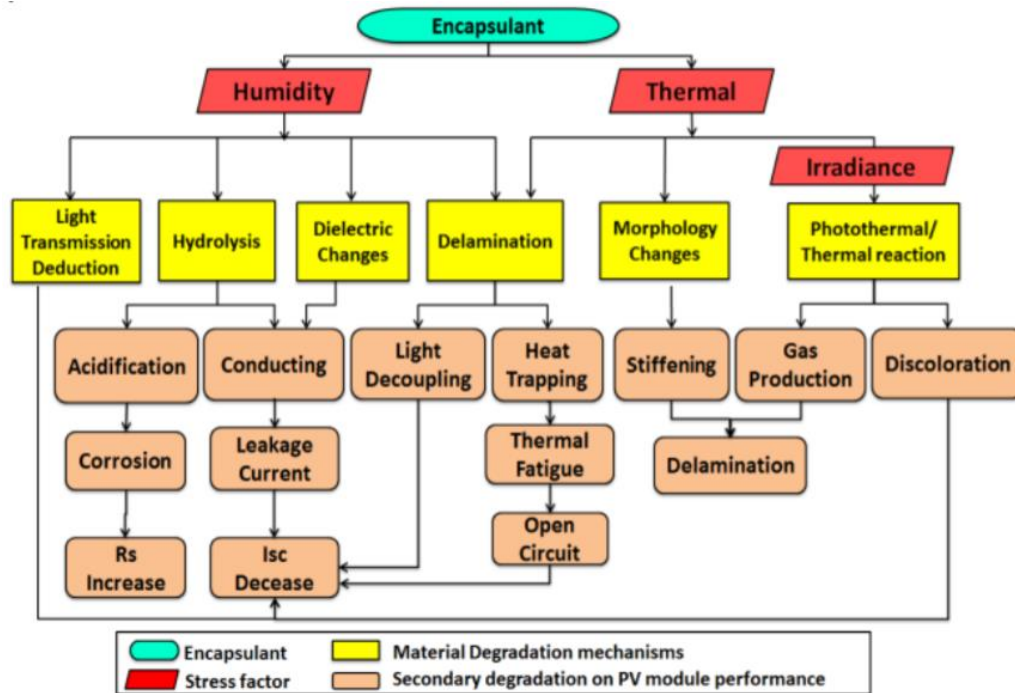
Figure 1.2: Impact of heat and humidity on the module components [3]

PV modules are tested for durability and reliability after their manufacture. The modules which do not pass the qualification test may not survive in the field for a more extended period. In the industry, to ensure they successfully thrive in the field, they are subjected to accelerated lifetime testing namely HALT (Highly accelerated lifetime testing) by the manufacturers before releasing the product. The lifetime testing aims to determine at what point the module will fail. If they fail prematurely, corrective actions are taken and stressed again to ensure premature failure does not occur and then released to the market.

In the lifetime testing care must be taken to ensure that the failures seen are the same failure modes identified from field exposure. For example, long-term ultraviolet (UV) testing at high temperature with humidity to evaluate material discoloration and

degradation could better be performed on small 1-cell or 4-cell mini-modules of the same cross-sectional construction as the full-size commercial module. Usage of step stresses in which the initial stress starts with the stress level from the qualification test and increases until failures are seen [7]. To obtain 25 years of field data in a few months of accelerated testing, high irradiance of 4-5 suns, few research groups around the world including ASU's Photovoltaic Reliability Laboratory (ASU-PRL) are currently utilizing UV lamps.

A range of nondestructive characterizations is performed to find out the performance of the module. In this thesis, tests are done before the start of the accelerated testing and after the accelerated test completion. The current-voltage (IV) measurements give various performance parameters including short circuit current and power of the PV module. The yellowness index provides information about change in the visible light absorption property of the encapsulant: basically, this study gives the information if the light transmittance of the material has degraded or not. The UV imaging provides early details on the browning and delamination before even before it can be detected in the visible light. These tests are carried out before and after the accelerated testing to see if the modules performance has dropped due to browning and delamination issues.

1.2 **Statement of the Problem and Project scope**

Hot-dry and hot-humid climates are prevalent in many locations where PV modules are installed. A choice of encapsulant which is least affected by environmental stressors is essential to operate in these climates. In this study, the UV-cut EVA based modules and UV-pass modules are subjected to combined stressors of UV and temperature replicating

hot-dry climate, and UV, temperature and humidity reproducing hot-humid climate. Extensive pre- and post-stress characterizations were performed to identify the degradation modes, determine the losses in performance parameters and to determine activation energies in each of the two stress tests. The project scope is depicted in the following flow diagram:
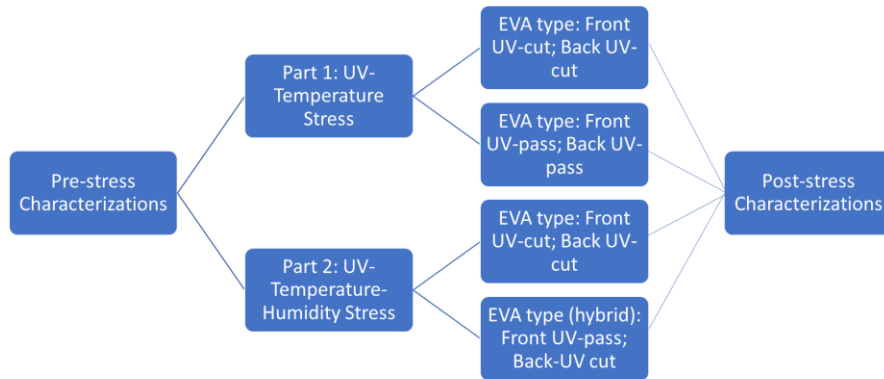
Figure 1.3: Scope of the project

1.3   **Thesis Objective**

The main objectives of this study are as follows:

- Identify the degradation modes of UV-cut and UV-pass EVA based modules under UV-temperature stress conditions.

- Identify the degradation modes of UV-cut and UV-hybrid EVA based modules under UV-temperature-humidity stress conditions.

- Determine the loss of performance parameters due to the above degradation modes.

2   LITERATURE REVIEW

In the photo-thermal degradation of polymers, a common factor is the generation of free radicals that are produced at the "activation sites" of impurities, ultraviolet (UV)-excitable chromophores, and metal trace or ions in the polymers [8]. During weathering EVA degrades resulting in adhesion loss between components termed as delamination and yellowing which brings down the module efficiency [4].

The yellow-browning of the ethylene-vinyl acetate (EVA) copolymer encapsulant used in PV modules has resulted in significant power losses of over 50% of the initial power output. UV absorbers (UVA), UV light stabilizers, and antioxidants (AO) are commonly introduced into polymer materials to eliminate or reduce the rate of degradation reactions and hence improve their weathering stability for longer service life. The weathering-degraded yellow EVA films have lost the ultraviolet (UV) absorber, Cyasorb UV 531(R), and the degree of cross-linking (gel content) has increased [9]. The discoloration is due to interactions between cross-linking peroxide and stabilizing additives and is also likely to be due to oxidation of the encapsulant [10].

Figure2.1:Degradation mechanisms in Ethylene Vinyl Acetate polymer under UV, Temperature[3]

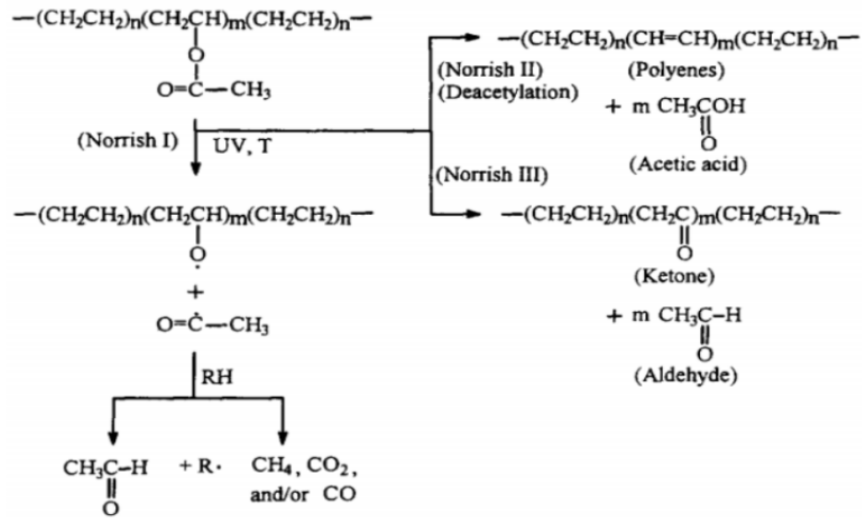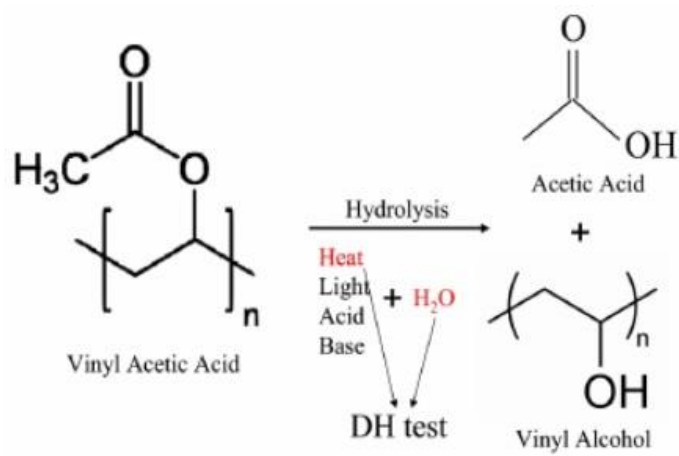
Figure 2.2:Degradation mechanisms in Ethylene Vinyl Acetate polymer under Heat and Humidity [11]

In addition to the decomposition of additives, the primary degradation reactions of EVA are deacetylation, hydrolysis, and photo thermal decomposition, which may lead to the evolution of corrosive degradation by-products, especially acetic acid [9]. These by-products, in turn, may accelerate metallization corrosion. Even minimal acetic acid production rates can have significant long-term effects when considering the 25 to 30 years of warranty that is being granted by the significant PV module producers nowadays since acetic acid can accumulate in front of the solar cells due to long diffusion paths to (and through) the back skin and affect the metallization on the front side [12].

Delamination can occur between encapsulant and glass or the cells and causes serious performance issues. Decoupling occurs in the light being transmitted reducing the number of photons the cell receives and results in reduced short circuit current (Isc). Delamination also weakens and interrupts dissipation of heat in the module causing thermal fatigue and, in some scenarios, open circuit reducing the power output. In thermal fatigue, recrystallization of the polymer occurs resulting in polymer stiffening and hence delamination [3].

Once the moisture inside the module permeates into EVA, it will form acetic acid which will attack the electric circuitry and, in the saturated case, free water may corrode cells as well. This will cause power reduction due to losses of passivation, electrochemical corrosion and ultimately lead to module failure[13].

The use of the slow-curing agent Lupersol 101 (L-IOI), which requires a curing time of-40-50 min at 145°C to produce 80% gel, is a significant factor responsible for an earlier and faster discoloration rate of EVA. The standard cure EVA contains Lupersol 101 peroxide as the cross linker. The discoloration appears to result from the interaction of additives in the presence of temperature and UV-with a combination of Lupersol 101 peroxide and other additives proving particularly troublesome [8].
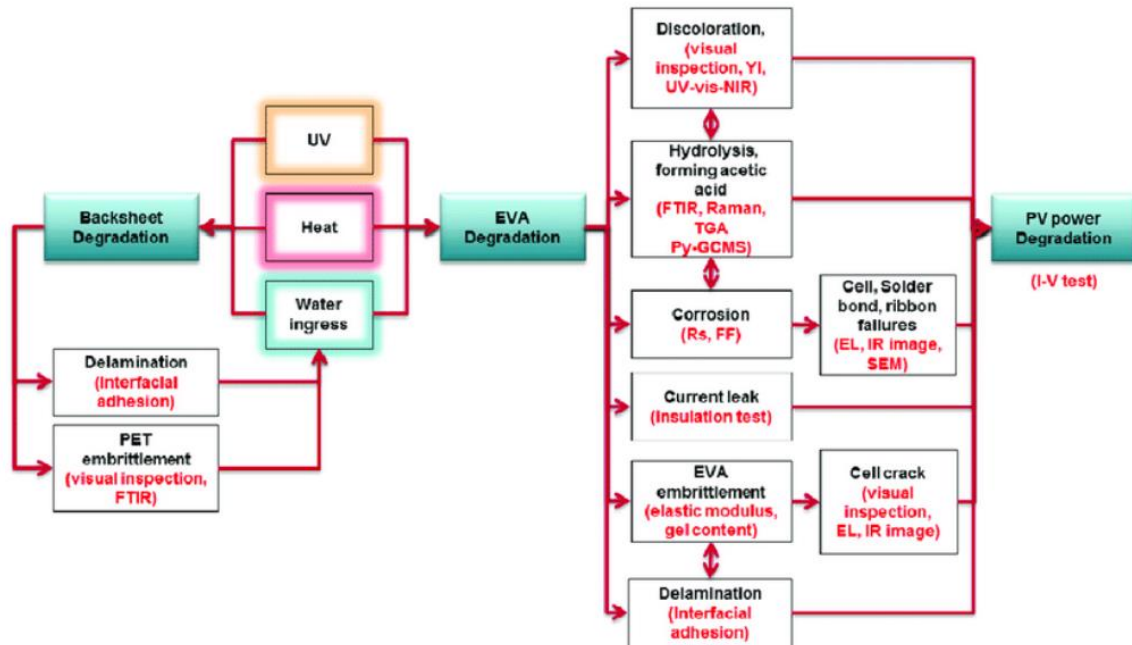

Figure2.3: Failure modes of PV modules caused by packaging materials and the evaluating approaches [14]

Photo discoloration reactions compete with photo bleaching reaction. On exposing dark brown EVA to air, the destruction of polyenic conjugation by photo-oxidation is observed. If air permeation is there from the beginning of UV light exposure, discoloration does not occur at all [8].

Debonding kinetics is affected by moisture in the environment resulting in lower adhesive energy. Peel tests conducted at an ambient temperature of 30°C and different conditions of relative humidity (RH) failure has been noted at the Titanium beam-EVA interface with reduced adhesive energy on increasing levels of humidity [15].

Adhesion loss and delamination occur on exposure to heat and moisture. In the accelerated testing, the delamination is often triggered by damp heat. Wu et al. studied reduction on peeling strength between EVA and back sheet in different conditions of damp heat. The decrease in peeling strength is dependent on the temperature and relative humidity. A model of humidity dose proposed assumes relative humidity at the back sheet surface to be the driving force and heat to be an accelerating factor by Arrhenius model[15].
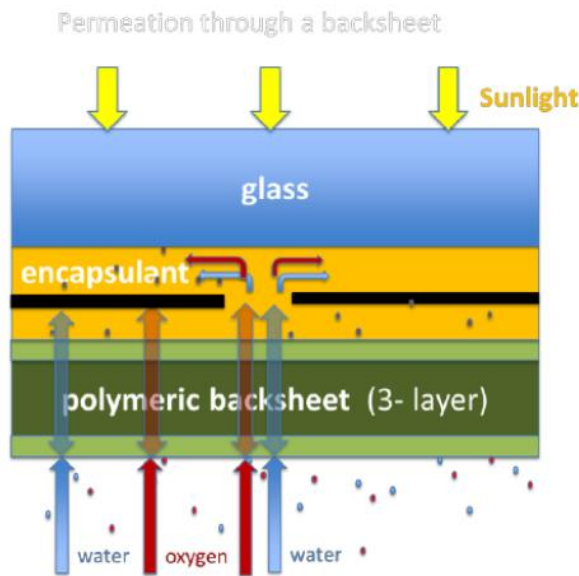

Figure 2.4 : Water and oxygen ingress path through the back sheet[16]

The moisture ingress in PV modules in Miami, Florida, has been correlated with failure rate, especially in hot and humid (damp) conditions (King et al. 2000). Investigations by Kempe (M.D. Kempe 2005) showed the rate of moisture ingress into PV modules and reported that the diffusivity of water has an Arrhenius dependence on temperature [17].

It is reported that in modules with a breathable back-sheet the moisture absorbed at night is desorbed during the day due to the higher temperature of the module and higher ambient water vapor pressure. However, the module can saturate in a rainy climate, especially when there is a drop in the temperature, which can be a problem owing to droplet formation by trapped water. Impermeable back sheet is a better moisture barrier; however, water can still penetrate and reach the center of the module in few years via the encapsulant [17].

Kim et al. studied the photo degradation behavior of EVA when exposed in a weathering chamber which has an inbuilt xenon arc lamp for irradiance. The induced photodegradation results in changes in the surface of polymer which is studied in terms of changes in the morphology and optical property variation. As a result of photodegradation, there is surface composition change as a result of oxygen introduction to the chain of the polymer, making the film hydrophilic aiding in water penetration [4].

Deepak Jain conducted a UV stress test on MSX mini-modules in the ATLAS Ci4000 chamber with a Xenon-arc lamp. The test conditions were irradiance setting 1 W/m^2/nm at 340 nm, 65% RH, 20°C chamber temperature. The activation energy for encapsulant browning is 26-44 kJ/mol (0.27-0.46 eV)[18].

14

3 METHODOLOGY

3.1 Module Construction

In this study two tests are carried out:

1. UV-Temperature testing (dry run with adhesive aluminum)

2. UV-Temperature-Humidity testing (with humidity and oxygen)

To make the test modules for study a monocrystalline silicon cell of 156 x 156 mm^2 dimension was selected. The cell is laser cut to nine pieces with each cell measuring 5.2 x 5.2 cm^2. The cells ribbons are soldered by soldering equipment. The nine cells are made into a mini module with the sequence: solite tempered glass 8 x 8 square inches, EVA, nine cell pieces having intercell distance as 1.1-1.2 mm, EVA, TPT (Tedlar-Polyester-Tedlar)back sheet. Two different kinds of EVA, UV-cut, and UV-pass were used for encapsulation. The UV cut EVA protect the cells by absorbing UV radiation lower than 360 nm. UV Pass allows the full spectrum of UV light to pass through the cell but, there is a risk of degradation of the back sheet [19].

For the dry UV testing, three modules of Glass/UV Cut EVA/solar cell/UV Cut EVA/Back sheet, and three modules of Glass/UV Pass EVA/solar cell/UV Pass EVA/Back sheet was used. The study aimed to study only the effect of UV light on the UV cut and UV pass encapsulants. Hence the back sheet of the modules was covered with adhesive aluminum foil to prevent oxygen and moisture ingress. Three different

temperatures for the two sets of modules with two different encapsulants was achieved by using foam board of varying thickness.

For the humidity testing in the UV chamber, six modules were used. Three modules of construction Glass/UV Cut EVA/solar cell/UV Cut EVA/Back sheet and three modules of construction Glass/UV Pass EVA/solar cell/UV Cut EVA/Back sheet construction (UV-Hybrid) were used. The back sheet is directly exposed to humidity/moisture and the front side to UV radiation as shown in *Figure 3.2*.
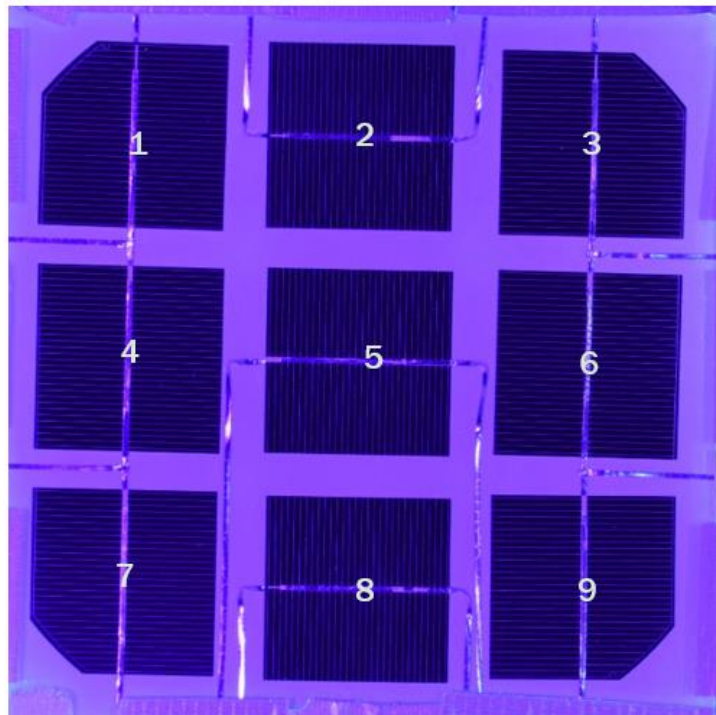

Figure 3.1: Cell numbering in the mini module

3.2 **Accelerated UV stress testing**

The primary cause of reliability failure in solar modules is because of delamination, encapsulant browning, and the modes which are primarily induced because of UV radiation. To simulate the outdoor conditions inside an accelerated chamber is essential. This helps to study the failure modes in a shorter period, and hence this helps the manufacturers to view the reliability of the material used. At ASU-PRL there are 144 UV lamps in a chamber capable of producing UV radiation with an irradiance uniformity of ±15% over the test plane of the module(s) with no apparent irradiance at wavelengths below 280 nm. There is an irradiance sensor which measures the irradiance of the UV light produced by the UV light source at the test plane of the module(s), within the wavelength ranges of 280-320 nm and 320-400 nm with an uncertainty of ±15% or better. Irradiance measurement is done using a calibrated radiometer at a proposed module test plane. As per the IEC 61215 standards the irradiance should not exceed 250 W/m2 (about five times natural sunlight level) at wavelengths between 280-400 nm. Module temperature should be maintained within 60±5°C.

The UV radiation is up to 5 times the sun intensity to accelerate the test. The chamber is equipped with UV tube lights, a data acquisition unit, and temperature sensors. Global irradiance in the Arizona field at latitude tilt is 6.5 kWh/m^2 /day. Twenty-five years of outdoor exposure in this environment is equivalent to approximately 3000 kWh/m^2 considering UV exposure in Arizona is equal to 5% of 6.5 kWh/m2 /day which is 0.325 kWh/m2 /day. Hence with accelerated UV chamber at higher operating temperature than

17

the field operating temperatures, the outdoor conditions can be simulated in a shorter period, and the degradation modes and mechanisms can be studied. If an UV chamber works for 24 hours a day at 250 W/m^2 irradiance at 60°C and if the fielded PV module operates at 40°C at 6.5 sunhours per day with 5% UV irradiation, then 25 years of UV effect in the field can be obtained in about four months UV exposure in the UV chamber assuming an activation energy of about 0.6 eV for the degradation reaction of encapsulant.
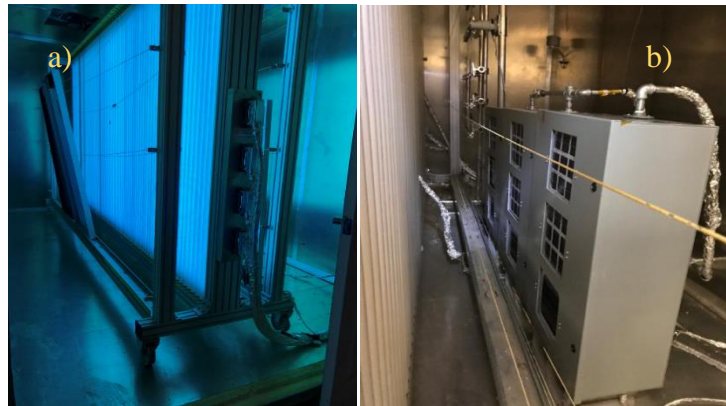

Figure 3.2:a) Inside view of alighted UV chamber b) RH box placed in front of the UV lamps

For the dry UV test, the modules were directly exposed to UV on the front side and the backsheet and edges of the laminate were covered with adhesive aluminum tape to avoid air/oxygen and water vapor transmission through the backsheet. Therefore, in this dry setup, EVA is exposed to only UV and temperature with no access to oxygen or humidity. The temperature of the module was measured by a T-type thermocouple attached to the back sheet directly behind the fifth cell of each module.

3.3 **UV-T-H OPERATION**

The UV-T-H (UV-Temperature-Humidity) setup consists of a steam generator which delivers humidity in the form of low temperature steam inside a stainless-steel enclosure having a heating blanket and humidity sensor. The overall setup contains three enclosures to maintain three different temperatures. Each enclosure contains three windows and each windowcan accommodate one 9-cell module shown in*Figure 3.2*. In the current study, we needed only two windows (one for UV Cut EVA and the other for UV Hybrid EVA) and the third window was not needed. The third window was covered with a dummy 1-cell module to avoid the loss of humidity through the unused windowas shown in*Figure 3.3*. Temperature is one of the three stressorsused in the experiment and the other two stressors are UV and humidity. Three thermal blankets were used to maintain three different temperatures in the three enclosures as shown in*Figure 3.4*. The thermal blanket is kept at 9.25 inches from the 9-cell test modules.The required humidity and temperature inside the enclosure is maintained using a temperature and humidity controller along with a power supply as shown in*Figure 3.5* and *Figure 3.6*.The RH is monitored with humidity sensor HX 171 manufactured by OMEGA. The module temperature is monitored with a K-type thermocouple attached to the backsheet of each module at the center of the fifth cell shown in *Figure 3.1*. The data acquisition system collects the readings every ten seconds. Hence, in this setup, the UV light reaches the front side of the modules, and the back sheet is exposed to heat from the thermal blanket and humidity from the steam generator.
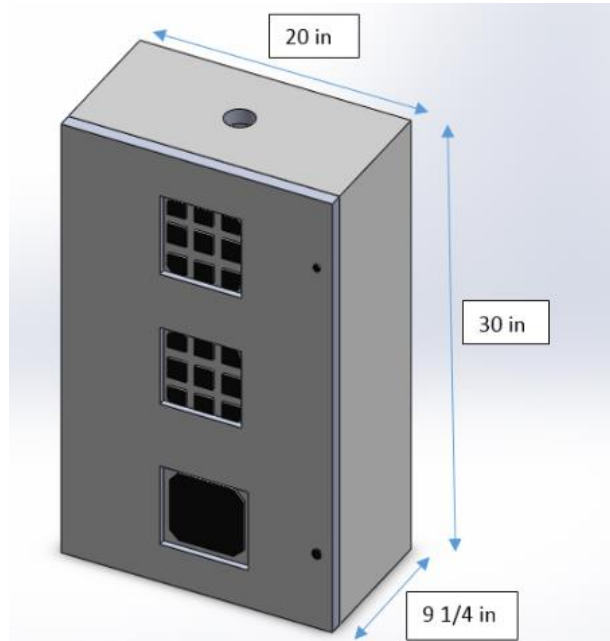
19

Figure 3.3: Dimensions of the box used for the UV-T-H testing (9-cell module testing shown in the top two windows and 1-cell dummy module testing shown in the bottom window; humidity is introduced through a hole shown on the top of the box)
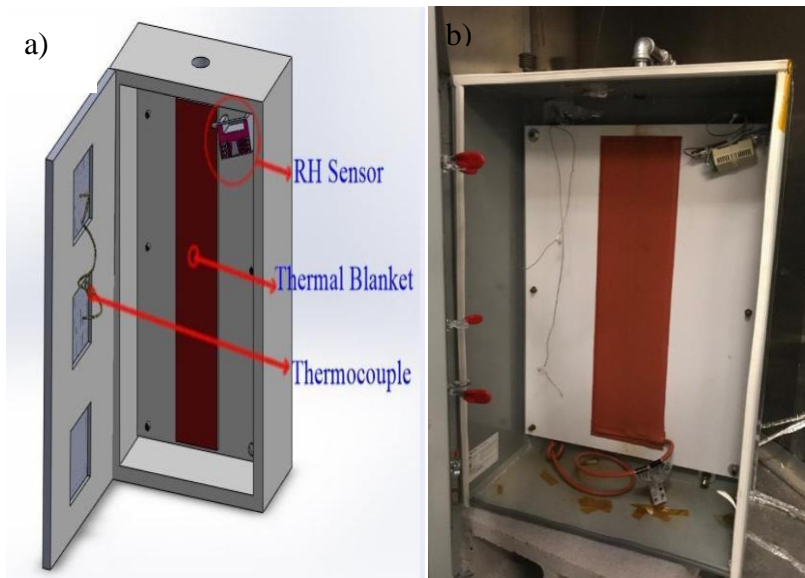
Figure 3.4:a)Components inside the T-H enclosure b) Photograph showing the location of heater and humidity sensor
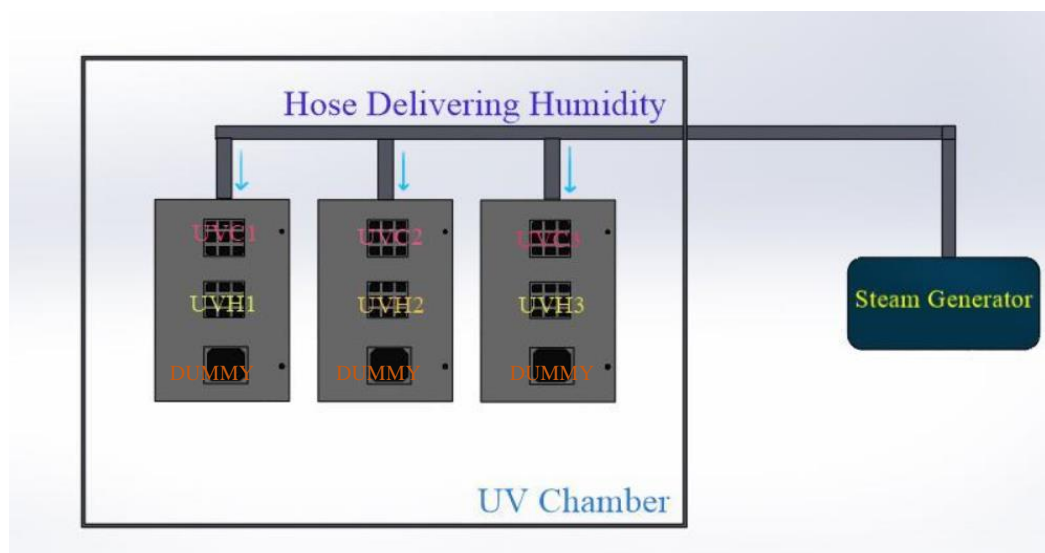

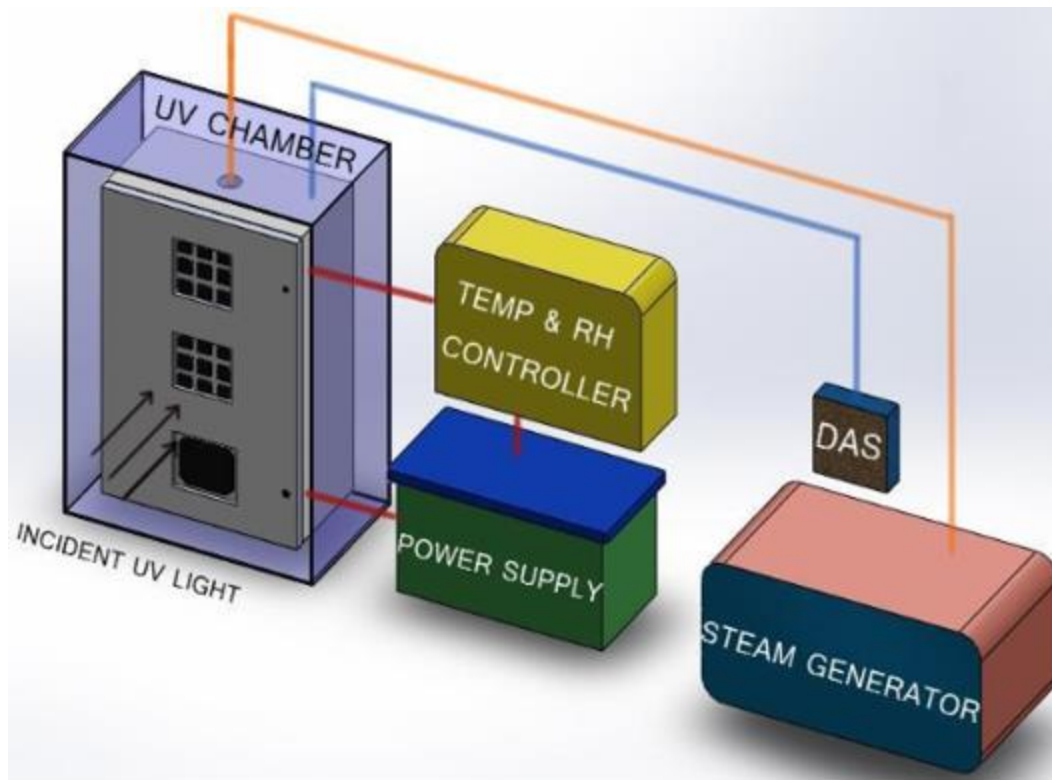Figure 3.5: Front view of the setup inside the UV chamber

Figure 3.6: Combined UV-Temperature-Humidity Setup (the power supply used for the heaters and the DAS can be used to monitor the temperature of individual cells in each module)

3.3.1 Steam generator

When the steam generator is switched on, there is steady steam production after 9 minutes when it's filled fully with water. This is equipped with a water level sensor which fills in water once the level drops below the required level. For the project, the steam generator serves as the source of providing humidity, allows steam, from which the values of RH are recorded using the humidity sensor.Nature steam generator of the model NTA 20 from TOULE SAUNA INC was used.

Figure 3.7: Steam generator for humidity delivery

3.4   Characterization techniques

3.4.1   IV Measurement

An indoor solar simulator is used for the IV measurements. The irradiance is calibrated using a PVM 798 reference cell. After the calibration, the test coupons are placed on the chuck. After opening the shutter, the light falls on the module of study. The measurements are taken for every test module through the ribbons coming out of each cell. From this, the value of short circuit current (Isc) of each cell is found, which is the primary parameter of study in this project.

Figure 3.8: Solar simulator for indoor IV measurements

3.4.2   UV Fluorescence Imaging

The UV-F imaging is used to detect the browning in the encapsulant much earlier than it can be recognized in the natural light. The imaging is done in the dark. The UV light is incident on the module of study from two arrays of UV lamps and the visible light thus

obtained from the test coupon is captured using a Nikon 3340 camera. The degraded molecules, i.e. the chromophores formed during the polymer degradation absorb the UV light incident, fluoresce and emit visible light which is longer than the wavelength of light absorbed. The fluorophore is a chemical compound which re-emits light on excitation and has aromatic groups or cyclic molecule with π bonds[20]. The setup provides uniform bright light on the module, and this technique offers fast characterization results.
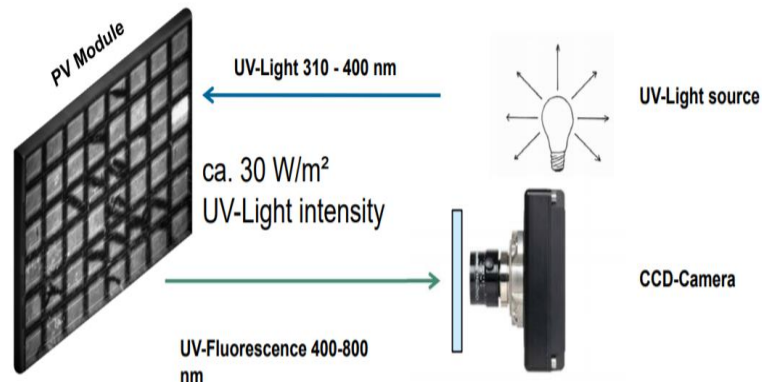
Figure 3.9: UVF imaging mechanism [21]

3.4.3 Reflectance Measurement

The amount of light reflected from the nine cell coupons is measured with a spectral radiometer. Before the data collection, the spectral radiometer is optimized. Optimization sets the proper settings for the light source which will be used to collect the spectra. The calibration is done on a white reference. The test coupons are measured for reflectance using a radiometer. The results are imported to the Viewspec Pro software and processed. Wavelength is plotted against reflectance in Origin after the processing.

25
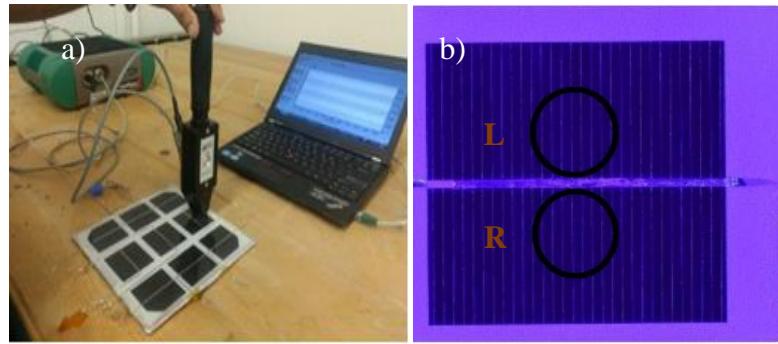
Figure 3.10:a) Reflectance measurement setup b) Positions in which the reflectance is measured

3.4.4 Colorimetry Measurement

The Xrite Ci 60 radiometer was used to measure the yellowness index. The PV modules have encapsulants which change their transmissive property over years of exposure. The encapsulants used in the PV modules start yellowing during field exposure. The YI measurements help to quantify the extent of yellowing in the PV modules. In this project, the measurements were helpful to quantify the change in the YI of encapsulants after exposure to combined stresses of UV, temperature, and humidity.
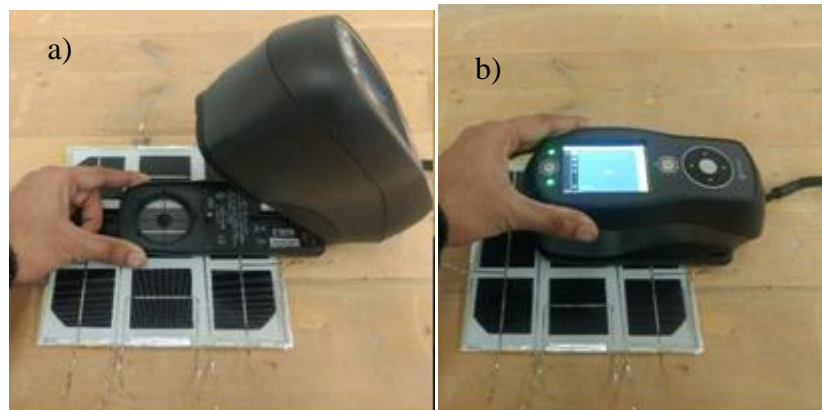
Figure 3.11:Colorimetry setup

3.5 Activation energy calculation

3.5.1 General Arrhenius equation

In this project the Arrhenius equation is used to determine the activation energy due to browning. To estimate the parameter a graph of 1/T vs ln (degradation rate) is plotted [19].

$$Rate\ of\ reaction = A * e^{\left(\frac{-E_a}{kT}\right)} \qquad (3.1)$$

$$ln(rate\ of\ reaction) = \left(\frac{-E_a}{k}\right) * \left(\frac{1}{T}\right) \qquad (3-.1)$$

k = Boltzmann's constant = 8.615 * 10-5 eV

K = Temperature in Kelvin

Ea = Activation energy in eV

4 RESULTS AND DISCUSSION

4.1 UV Fluorescence Results

The section is discusses the UV fluorescence imaging of the modules which were subjected to dry and humid testing conditions. The UVF imaginghas been carried out for the modules after 600 kWh/m^2 and 800 kWh/m^{2}of UV dosage for the modules in the dry run. For the humid run, the modules were characterized at 186kWh/m^2 and 200 kWh/m^2 of UV dosage. As discussedin*Pg15* the dry run consists of three modules with the UV cut encapsulant and three modules with UV pass encapsulant, respectively and their backsheet is covered with adhesive aluminum. To maintain three different temperatures foam boards of different thickness are used on the backside of each modules as explained in the thesis of Kshitiz Dolia [19]. The humid run consists of three UV Cut encapsulant and three UV Hybrid (UV pass in the front and UV cut in the back).

Figure 4.1 shows the UVF images of the coupons in the dry run. The images were taken at 600 kWh/m^{2}and 800 kWh/m^2.The images of 0,200 and 400kWh/m^2 were obtained from the previous set of experimental study by KshitizDolia.The UVF images can be correlated with the yellowness index measurement which is discussed in the upcoming result section. From the results, it can be visually seen that the intensity of yellowing is higher at 400 kWh/m^2. For the dry UV testing the backsheet was covered with aluminum foil so that the moisture and oxygen transport can be prevented to study the degradation mechanism with UV and temperature only excluding humidity. The expected result would be uniform browning/yellowing throughout the area of the cell as the bleaching

28

between the cells and the cell edges are prevented through the adhesive aluminum tape. However, from the UVF images, the periphery/edges of each cell in all the UV cut modules of study are not browned despite the adhesive aluminum cover even after an UV dosage of 800 kWh/m^2.

Based on UVF, a few of the cells were found to be cracked due to a fall after 600kWh/m^2 of UV exposure without the module shattering. Based on UVF, the EVA bleaching was found to occur along the cracks after 600 kWh/m^2 of UV exposure. There are three possibilities for these complementary observations:

    a. The generated acetic acid during UV exposure escapes through cracks and prevents catalytic assistance to the browning reaction. This possibility may not exist as the already browned EVA cannot get bleached though the browning cannot get worse than what was seen after 600 kWh/m^2 exposure.

    b. The thin aluminum foil is not thick enough to prevent oxygen transport through the foil at higher operating temperatures of the modules. This possibility may not exist either as the aluminum foil thickness was 100 micrometer much higher than 26 micrometers limit at room temperature [22].

    c. The physical attachment of adhesive tapes doesn't prevent oxygen seepage at the back sheet/aluminum interface because the adhesion strength of the tape becomes minimal at higher operating temperatures for all the modules

29

inside a dry UV chamber. It probably indicates that the aluminum tape shall be laminated, instead of physical attachment, during the fabrication of these mini-modules to completely avoid oxygen seepage at the back sheet/aluminum interface.

Based on the above arguments, we currently attribute the EVA bleaching at the cell edges and cracks to oxygen seepage along the backsheet/aluminum interface. This attribution is yet to be proven using OTR (oxygen transmission) measurements of the aluminum foil at different temperatures and using laminated aluminum foil in the fabricated modules.

Due to fall after 600 cells 2,3,9 in UVC4succumbed to cracks but did not shatter
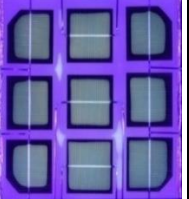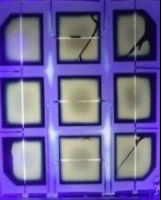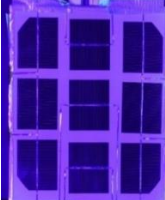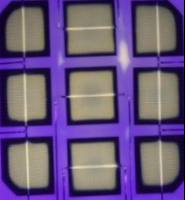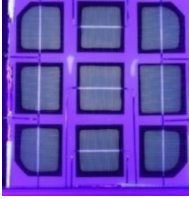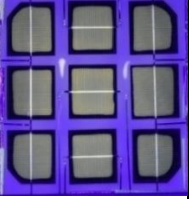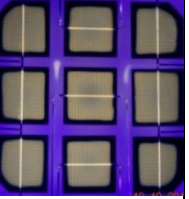
Module	UV Dosage (dry run adhesive aluminum)				
	0 kWh/m²	200 kWh/m²	400 kWh/m²	600 kWh/m²	800 kWh/m²
UVC4 60°C					
UVC5 69°C					
UVC6 73°C					

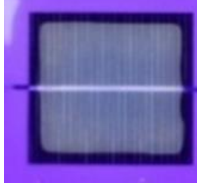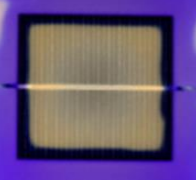Figure 4.1:UVF imaging of the UVC coupons of dry run at different dosage levels
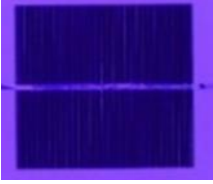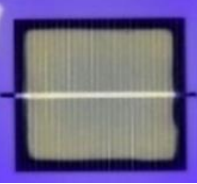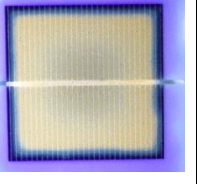
UVF image of cell 5 of coupon UVC-6 at different dosage levels				
0 kWh/m^2	200 kWh/m^2	400 kWh/m^2	600 kWh/m^2	800 kWh/m^2

Figure 4.2: UVF image of cell 5 of coupon UVC-6 at different dosage levels

In *Figure 4.3* there is delamination observed in the UVF image of the UVP modules of the dry run. This shows that the UVF image can detect the delamination in addition to the discoloration detection in the modules. At higher temperature, the delamination is more pronounced.
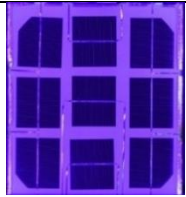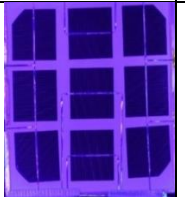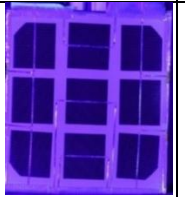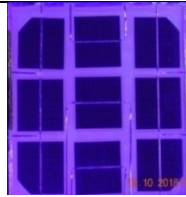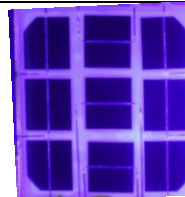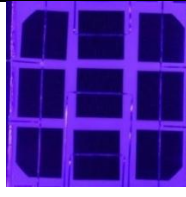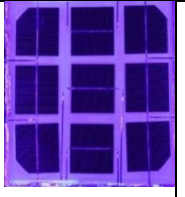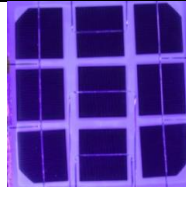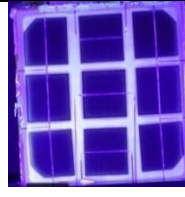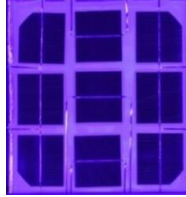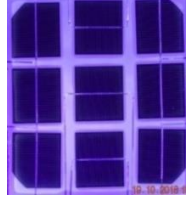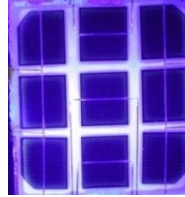
Module	UV Dosage (dry run without oxygen)				
	0 kWh/m^2	200 kWh/m^2	400 kWh/m^2	600 kWh/m^2	800 kWh/m^2
UVP1 59°C					
UVP2 67°C					
UVP3 69°C					

Figure 4.3: UVF images of UVP mini-modules at different temperatures andUV dosage
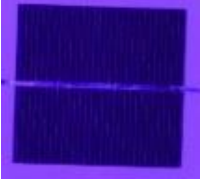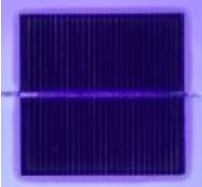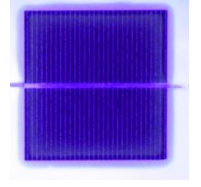
UVF images of cell 5 of UVP-3 at different dosage levels				
0 kWh/m^2	200 kWh/m^2	400 kWh/m^2	600 kWh/m^2	800 kWh/m^2

Figure 4.4: UVF images of cell 5 of UVP-3 at different dosage levels

Thereis a spread of white-brown color through the area of the cells at 800 kWh/m^2.Hence delamination is observed in the initial stages and at the later stages in addition to delamination there is discoloration observed too. The delamination could be a possible result of EVA lacking several adhesion promoters, or the adhesion promoters degrading with higher UV dosage.

The

Figure 4.5shows the UVF imaging of the UV cut coupons subjected to humidity testing. In comparison to the dry UV test the browning intensity is less intense and area is lesser compared to the dry run. This is because of the combined effect of humidity and oxygen which permeate through the backsheet.
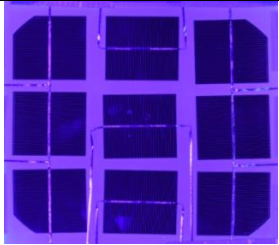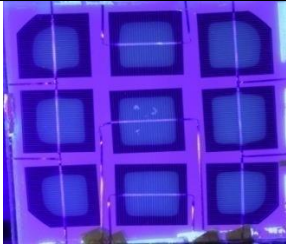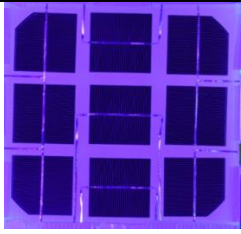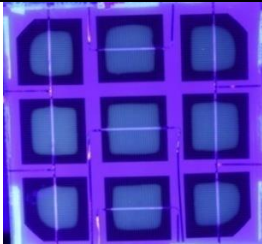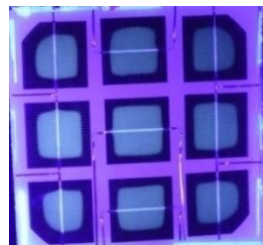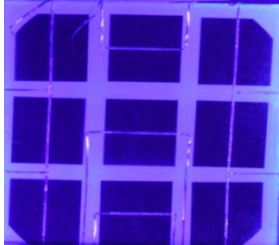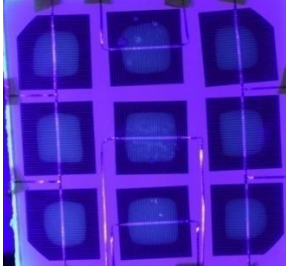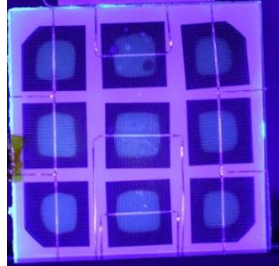
UV-cut Mini-module	UV dosage (humid run with oxygen)		
	0 kWh/m^2	186 kWh/m^2	200 kWh/m^2
Low T 59.93°C			
Mid T 64.15°C			
HighT 67.03°C			

Figure 4.5: UVF images of UVC-Humid coupons in the humid run at various dosage levels
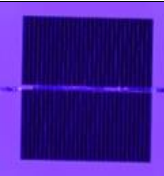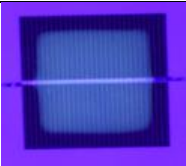
UVF image of cell 5 in Low T UVC coupon (humid run)		
0 kWh/m^2	186 kWh/m^2	200 kWh/m^2

Figure 4.6: Close-up UVF image of cell 5 in Low T module at various dosage levels

From *Figure 4.6* the intensity of discoloration increased with an increase in the UV dosage.
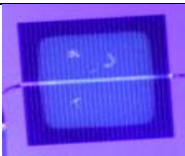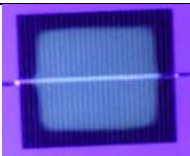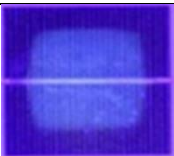
UVF image of cell 5 at 200 kWh/m2 at various temperatures (humid run)		
Low T 59.93°C	Mid T 64.15°C	High T 67.03°C

Figure 4.7: Close-up UVf image of cell 5 at 200 kWh/m^2 at various temperatures

From *Figure 4.7* the cell 5 of coupons at three different temperatures are shown. A difference in the area of browning is observed. There are two possibilities

1) It could be due to different values of humidity

   The three modules were maintained at RH 18%, 30% and 50%. No matter high the humidity is, the back sheet will absorb moisture only to a certain limit depending on its water vapor transmission rate (WVTR).WVTR depends on the material of the back sheet, the diffusion coefficient of the back sheet.

2) Higher oxygen diffusion rates with higher temperatures. With the increase in temperature, a lower browning area is observed. Hence, we can conclude that at higher temperatures, there is more upper oxygen diffusion and therefore the browning vicinity is likewise smaller. With lower temperatures,owing to lower oxygen diffusion rate there is a higher browning area.

The*Figure 4.8*shows the UVF imaging of the UVhybrid modules. The modules have UV pass EVA in the front and UV cut encapsulant in the backside. By the dry humidity testing of the UV Pass coupons, delamination was observed at UV dosage of 200kWh/m^2. Hence in this scenario also, delamination was the expected degradation mode in the front.

UVH Mini-module	UV dosage (humid run with oxygen)		
	0 kWh/m^2	186 kWh/m^2	200 kWh/m^2
Low T 56.06°C			
Mid T 60.8°C			
High T 63.18°C			

Figure 4.8: UVF images of UVH coupons in the humid run at various dosage levels

The cells in the module showed a ring pattern.Basically, UVpass encapsulant in the front side is not discolored at the centers of the cells and the edges of the cells but discolored between the cell-center and cell-edge forming a discolored ring.

According toresearchers from NREL,the following explanation maybe able to describe the ring pattern. At 0 kWh/m^2 dosage, the cell is clear from discoloration degradation mode.

1) After the start of the experiment, there is both oxygen and humidity transport through the backsheet. Since the molecular weight of water vapor is lower than oxygen gas, itcould diffuse faster through the backsheet and hydrolyzefront EVA resulting in acetic acid production catalyzing the browning reaction of some additives in the front EVA (by grahams law of diffusion the rate of diffusion is inversely proportional to the molecular masses). As a result, the encapsulant over the cell edges will be browned starting from the cell boundaries, and the discoloration pattern travels toward the center.

2) But, the competing bleaching reaction from oxygen diffusionoccurs at a slower rate than water. Oxygen, when it permeates through the backsheet, bleaches the cell browned area on the periphery leading to ring formation. The diffusionrate of oxygen is not enough to ingress further into the cell area and thus bleach the discolored ringcaused by moisture ingress. Hence the ring pattern is formed.
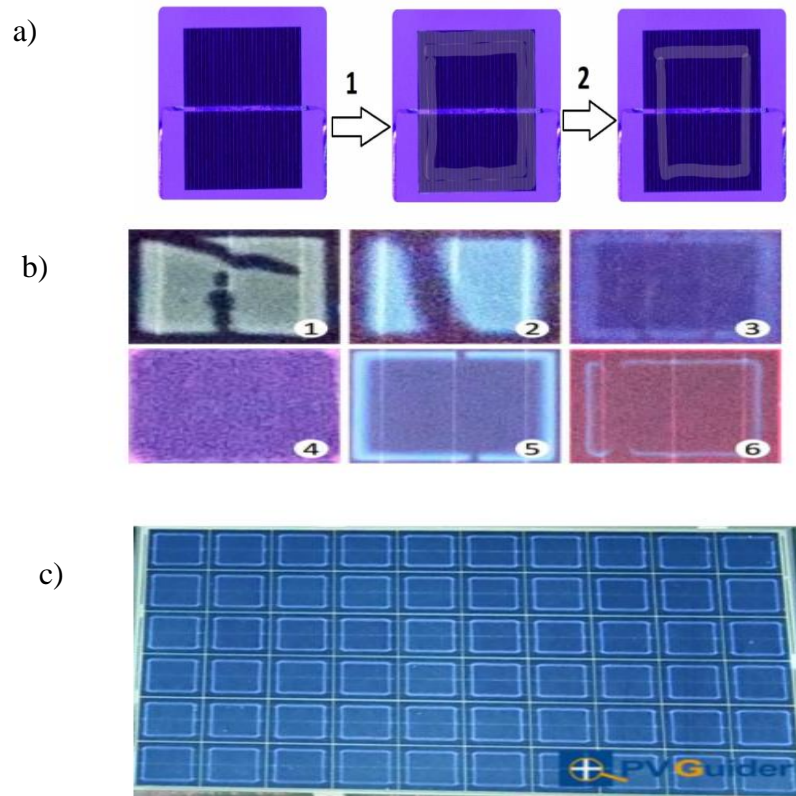
Figure 4.9:Possible mechanism of ring discoloration formation in a hybrid module (front UVpass and back UVcut) b) Discoloration pattern observed in solar fields in south eastern US[23] c)Module showing the ring pattern[24]

Another possible explanation is that UV cut encapsulant is used on the backside. The UV cut encapsulant has UV absorbing additives. There is a possibility that the additives degrade resulting in fluorophores and they migrate from the backside encapsulant (which does contain UV inhibitors) to the front side. But the migration may not be true because the UV absorbers are macromolecules. It is difficult for the macromolecules to migrate to the front side.

Figure 4.9: was reported by the southern company that modules with ring fluorescence were observed in the Southeastern US. They reportno geographic dependence and it seems to be a phenomenon arising in younger modules (i.e. more recently manufactured and exposed for less time).

The researchers hypothesize that there may be some dependence on moisture (i.e. humidity) but have no firm basis for that. More controlled experiments on a statistically significant number of samples where the various possible environmental stimuli are varied, and the fluorescence of the front and rear EVA are imaged will be ultimately necessary to explain the phenomenon.

Multiple sites of various ages and manufacturers have been inspected. A subsample of resultsare shown in *Figure 4.9b*. Plants with older modules exhibit a square UVF pattern, while mostyounger modules exhibit a ring[23].

Hybrid: UVF image of cell 5 in Low T module		
0 kWh/m^2	186 kWh/m^2	200 kWh/m^2
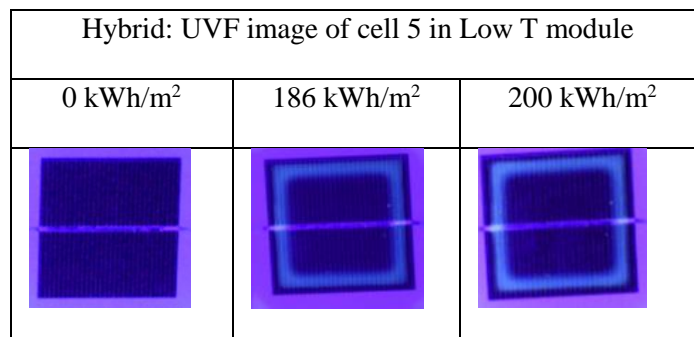
Figure 4.10: Close-up UVF image of cell 5 in Low T module at various dosage levels
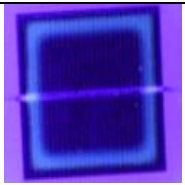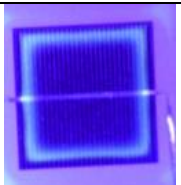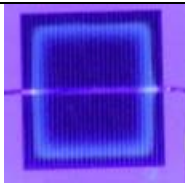
Hybrid: UVF image of cell 5 in Low T module		
56.06°C	60.8°C	63.18°C

Figure 4.11: UVF image of cell 5 in Mid T module at various temperatures

In the hybrid coupons as shown in the *Figure 4.11*, visually the ring area is higher at lower temperatures. Also, in this, we can see there is more bleaching in the periphery at a higher temperature, less bleaching at the boundary at a lower temperature due to reduced oxygen diffusion showing there is more oxygen bleaching at a higher temperature.

4.2 **YI Results**

The *Figure 4.12*shows the ΔYI values of the UV-Cut module in the dry run. From the graph below the decreasing order of ΔYI is UVC6<UVC5<UVC4. On correlating the UVF images with the YI measurements the greater the intensity of discoloration the greater the yellowness index. Also, the yellowness index increases with an increase in temperature with UVC-6 showing greater ΔYI.
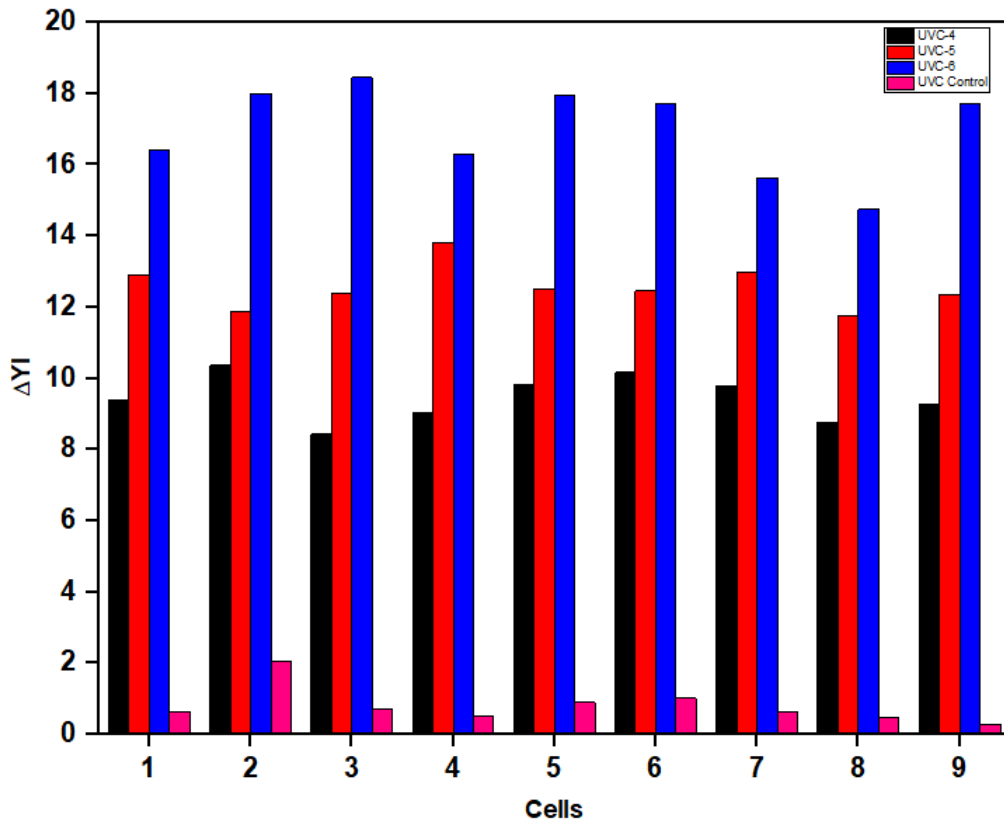
Figure 4.12: ΔYI of all cells for the UVC modules

The *Figure 4.13* shows the ΔYI of the UV Pass modules. The change is ΔYI is negligible compared to the UV Cut modules. From the UVF images of the UV Pass coupons at 800 kWh/m^2 there was delamination with slight browning around periphery. The occurrence of light discoloration is supported from the positive values of ΔYI in some cells when compared to the negligible values of ΔYI for the control modules of UV Pass encapsulant.
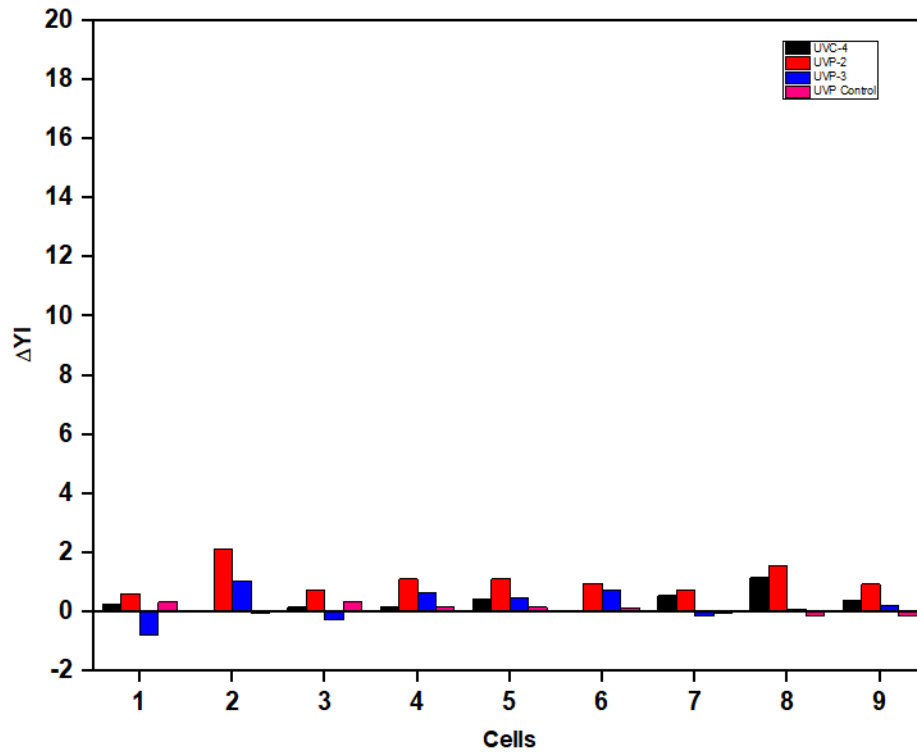
Figure 4.13: ΔYI of the all cells for the UVP modules

The*Figure 4.14*shows the variation of average YI of each module with the UV dosage. With increase in the UV dosage the value of average YI increases. This can be attributed to the formation of UV excitable chromophores which form on degradation of EVA with continuous UV dosage.

The variation of the averageYI in the UV Pass module with the UV dosage is also shown in *Figure 4.14*. With increase in dosage there is no significant YI increase for the UVP modules because of lack of intense discoloration.
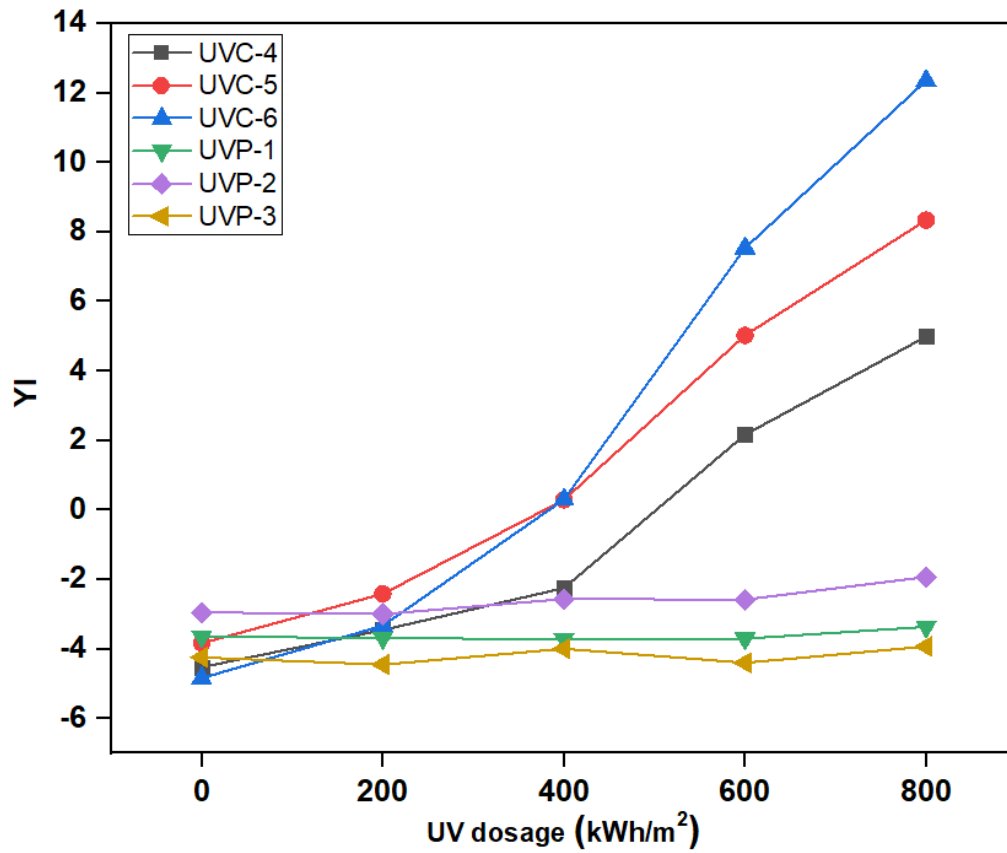
Figure 4.14:Change in average YI of the UVC and UVP modules with UV dosage

.
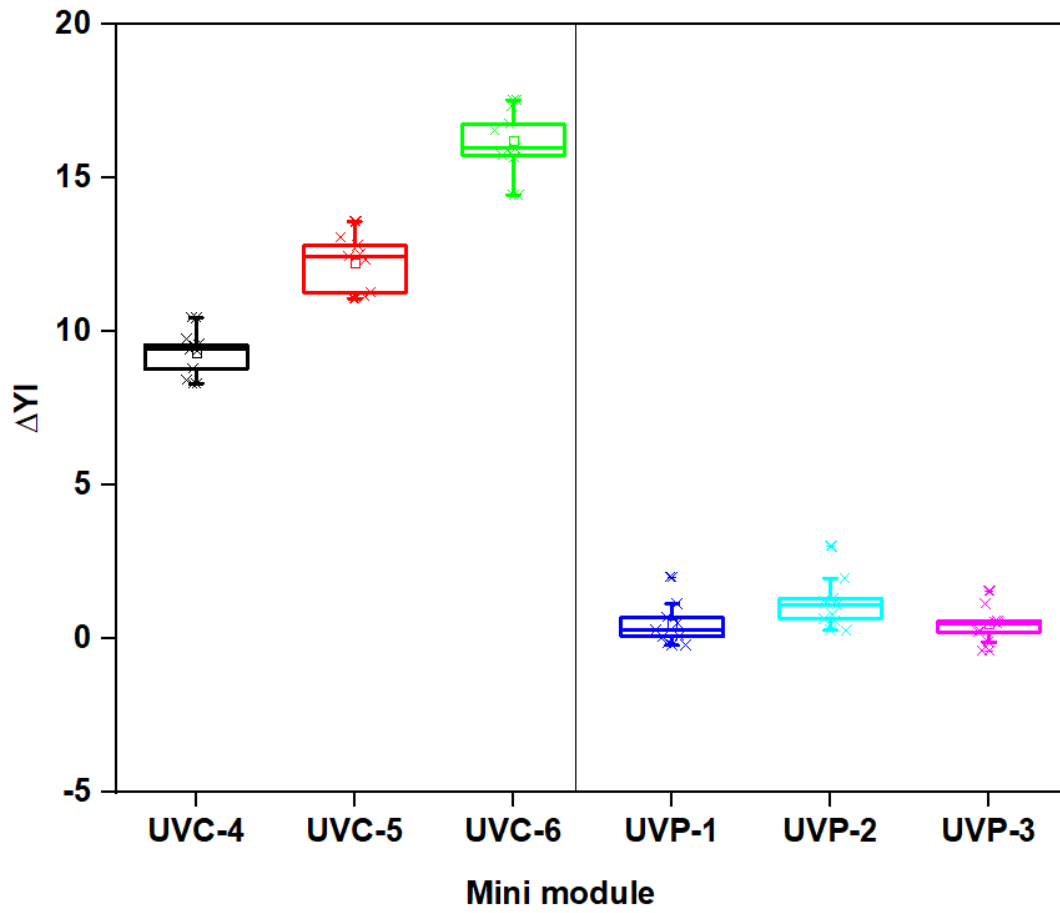
Figure 4.15: ΔYI of modules after 800 kWh/m^2 UV exposure in the chamber testing at low, mid and high temperatures.

The ΔYI increases with an increase in the module operating temperature for the UV cut modules. Since there is no yellowing in the UV Pass coupons the YI change is negligible and cannot be studied with temperature.

The*Figure 4.16*shows the ΔYI for theUVcutmodules in the humid run. Three different temperatures were achieved.As discussed earlier,since the backsheet is permeable to oxygen and moisture, the discoloration changes according to the extent of diffusion of water and oxygen.
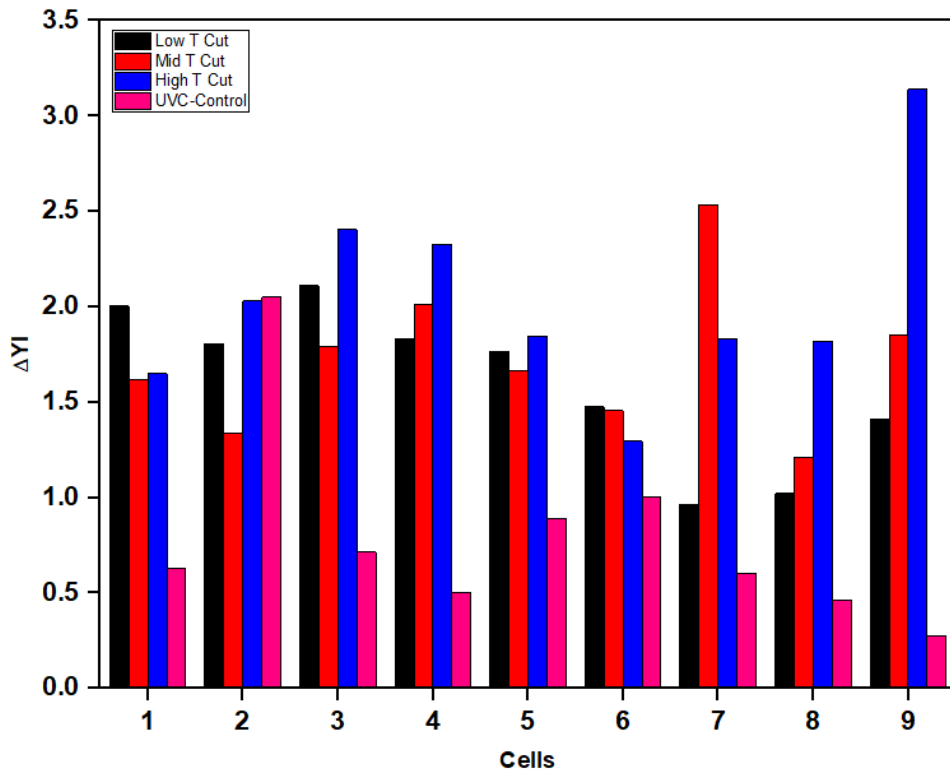
Figure 4.16: ΔYI of the all cells for the UVC modules in humid run

The*Figure 4.17*shows the ΔYIvariation with for the UV hybrid coupons. The ring pattern was observed near the periphery and the area inwards from the ring was lightly discolored. The UV-Pass encapsulant was used in the front side. From *Figure 4.13* the UVP modules show negligible change in the value of ΔYI. But in this case the ΔYI is positive even at dosage of 200 kWh/m^2 dosage strongly supporting the phenomenon explained in*Figure 4.9*.
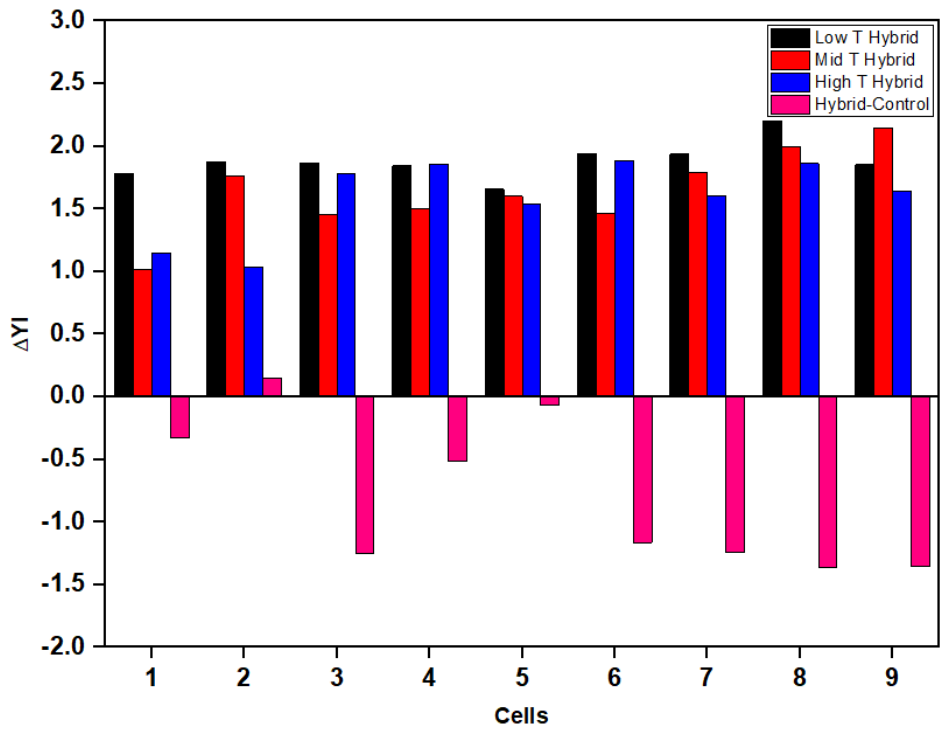
Figure 4.17: ΔYI of the all cells for the UVH humid coupons
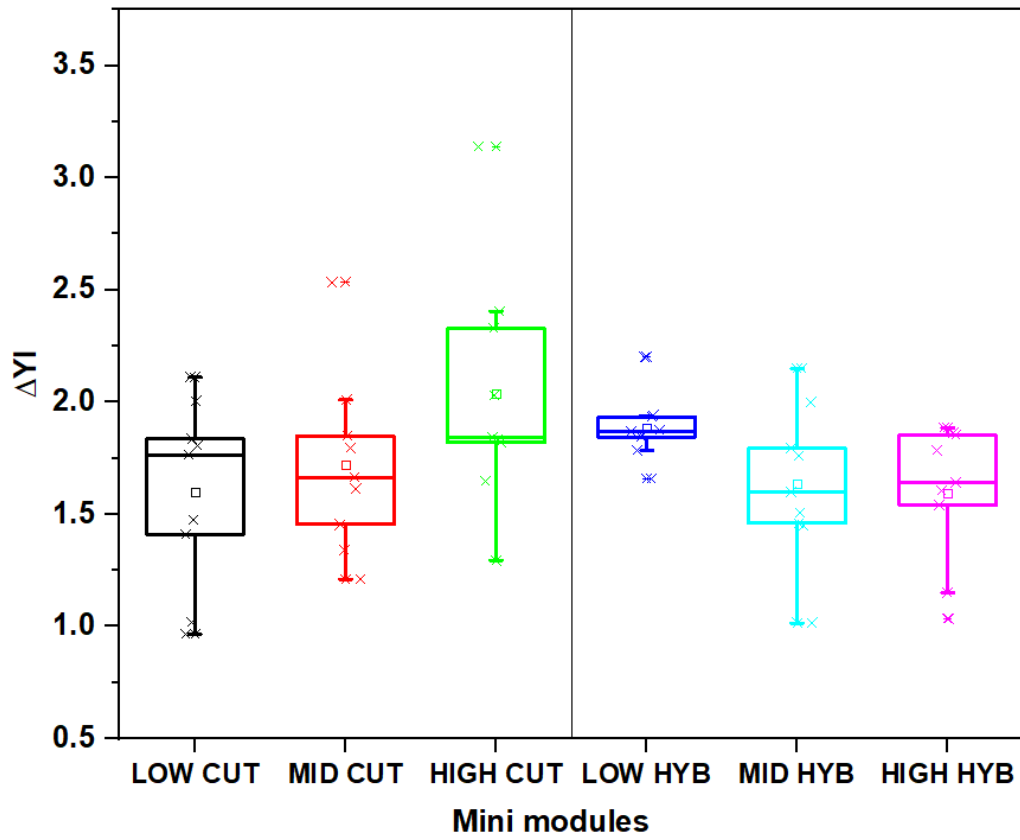
Figure 4.18: ΔYI of coupons after 200 kWh/m^2 UV exposure in the chamber testing at low, mid and high temperatures

From the *Figure 4.18*, a trend with temperature cannot be observed because of the combined effect of Temperature and humidity.

4.3   **IV Results**

The IV measurements for the coupons are done using an indoor solar simulator. The measurements for the humid coupons were carried out at 0 and $186kWh/m^2$. For the dry coupons it is carried out at $600kWh/m^2$. The variation of the Isc degradation rates for different coupons is shown in *Figure 4.19* and *Figure 4.20*

In the humid run, the degradation of Isc is less than 1% for the coupons with UVC encapsulant. This shows that the light discoloration observed in the UVF imaging does not contribute to the Isc degradation. The Isc degradation of the UV hybrid coupons is higher than 2% showing the UV-Hybrid coupons might not be well suited for field applications. The drastic drop in the Isc of the UV-Hybrid modules might be because of the ring pattern showing it might be detrimental to the module performance.

In the dry run, for the UV cut modules browning was observed. Hence the Isc degradation observed is attributed to the reduction in transmission of the visible light due to browning. The degradation increases with increase in temperature. In the UV-Pass modules delamination was observed from the UVF images. The degradation in Isc of the UV-Pass coupons can be attributed to delamination and the initiation of light discoloration. Moreover, the change in YI is negligible but the Isc loss is drastic which could be possible due to delamination.
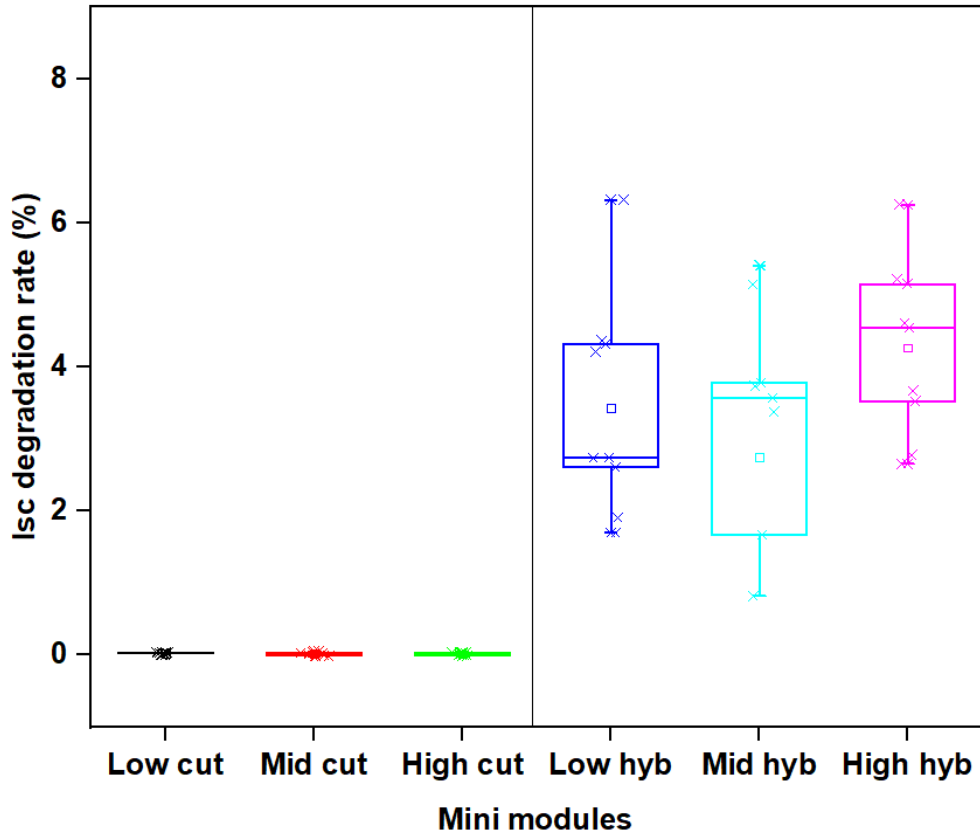
Figure 4.19: Change in the Isc degradation rate of the modules in the humid run
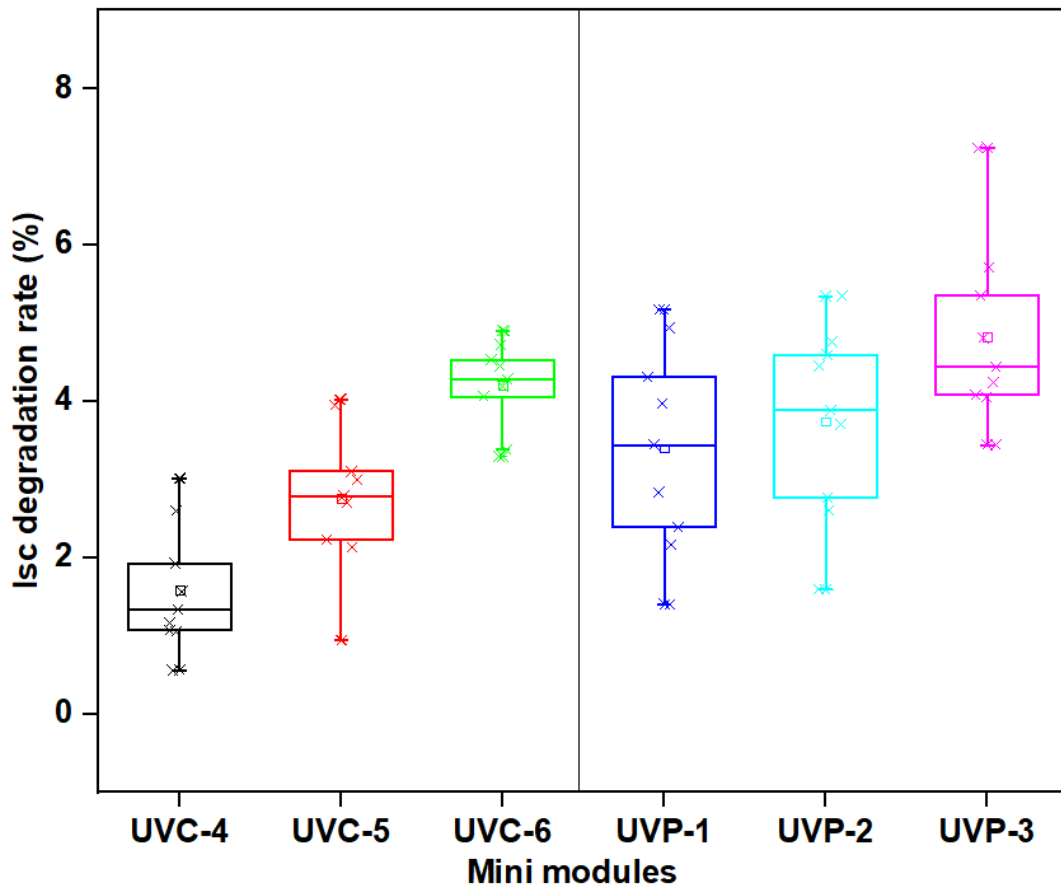
Figure 4.20:Change in the Isc degradation rate of the coupons in the dry run

4.4 **Reflectance Result**

The reflectance pattern for the UV cut module in dry conditions at 0 kWh/m^{2}and 800 kWh/m^{2}are shown below. The reflectance measurements are carried out on either side of the busbar (L and R) of each cell to increase the reliability of the results (*Figure 3.10*).
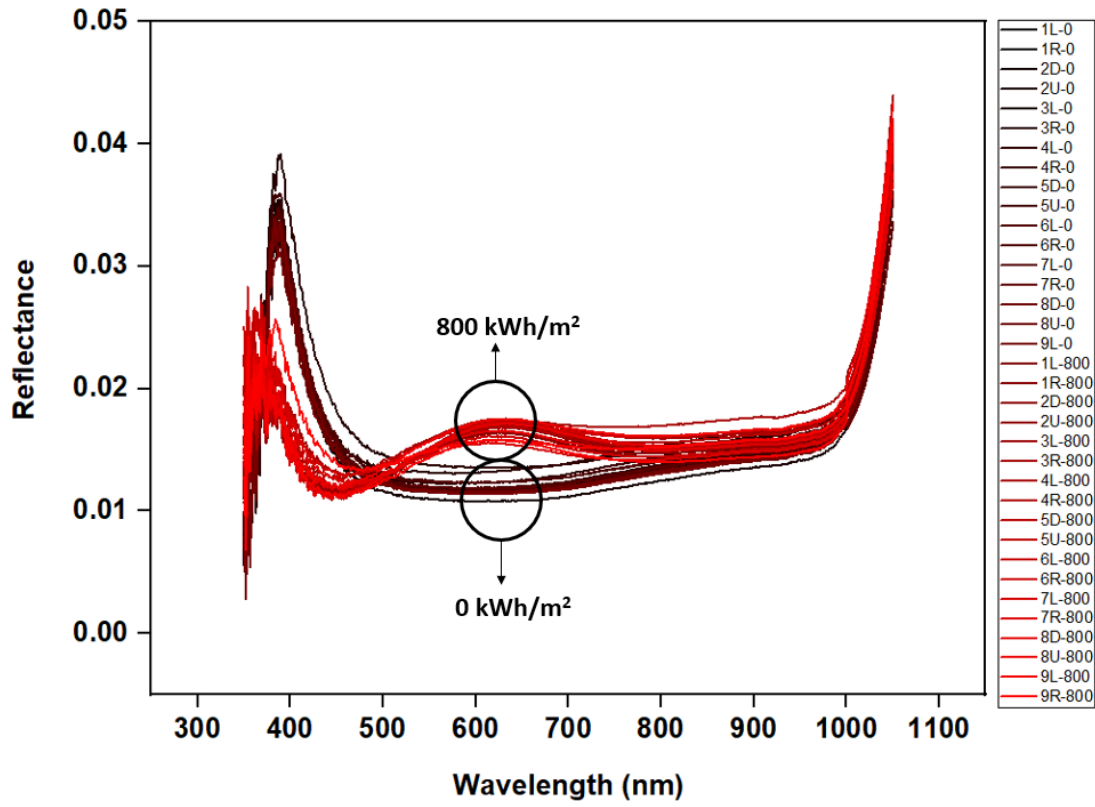
Figure 4.21:Reflectance plot for all cells in UVC-6 (dry run)

The spectral reflectance is high for the discolored EVA when compared to the module with fresh and unexposed EVA. This trend is more prominent at dosage from 450 nm to 800 nm.The increased reflectance is because of browning, reducing the visible light transmitted to the cell and thereby affecting the power[25]. This also indicates the degradation of the antireflective coating with the loss of UV absorbers.
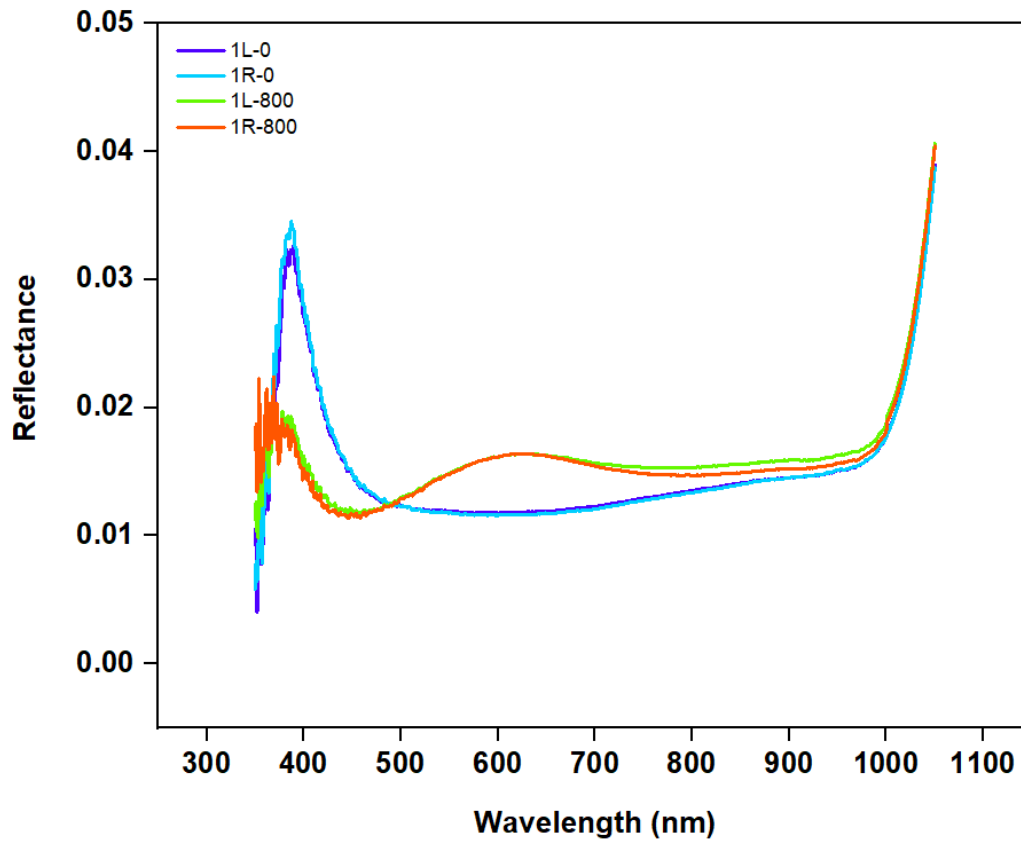
Figure 4.22:Reflectance for cell 1 at positions L and R of UVC-6 at 0kWh/m^2 and 800 kWh/m^2

However, reflectance of discolored EVA was lower than that of EVA without discoloration in wavelength 350–400 nm. That can be attributed to the loss of ultra violet absorbers in EVA with higher UV dosage[25]. This can also indicate that the antireflective coating of the module is more prone to UV damage with the loss of UV absorbers and hence results in increased reflection in the range of wavelength from 450 nm to 1100 nm.
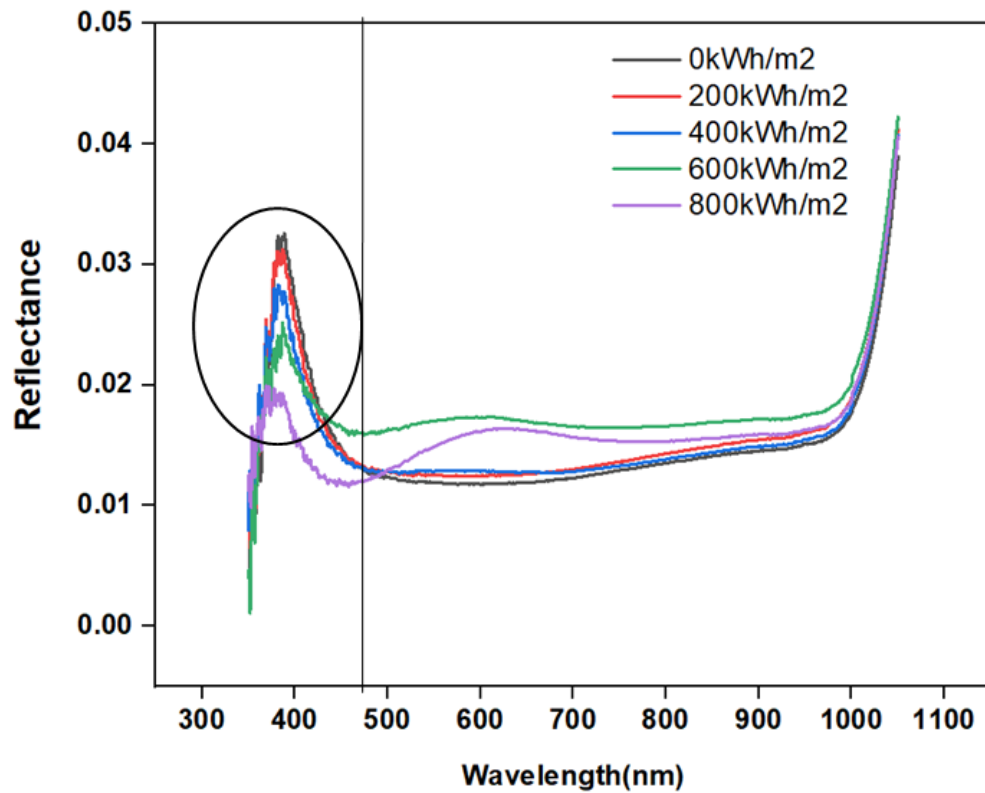
Figure 4.23:Reflectance study at 1L position from 350 nm to 400 nm of UVC6 (high T dry coupon)

56

Delamination is a major problem because it can lead to two effects: light decoupling where reflection increases. The reflectance at 800 kWh/m^{2}is higher than the reflectance at 0 kWh/m^2 which is due to increased reflectance as shown in *Figure* 4.25[25].
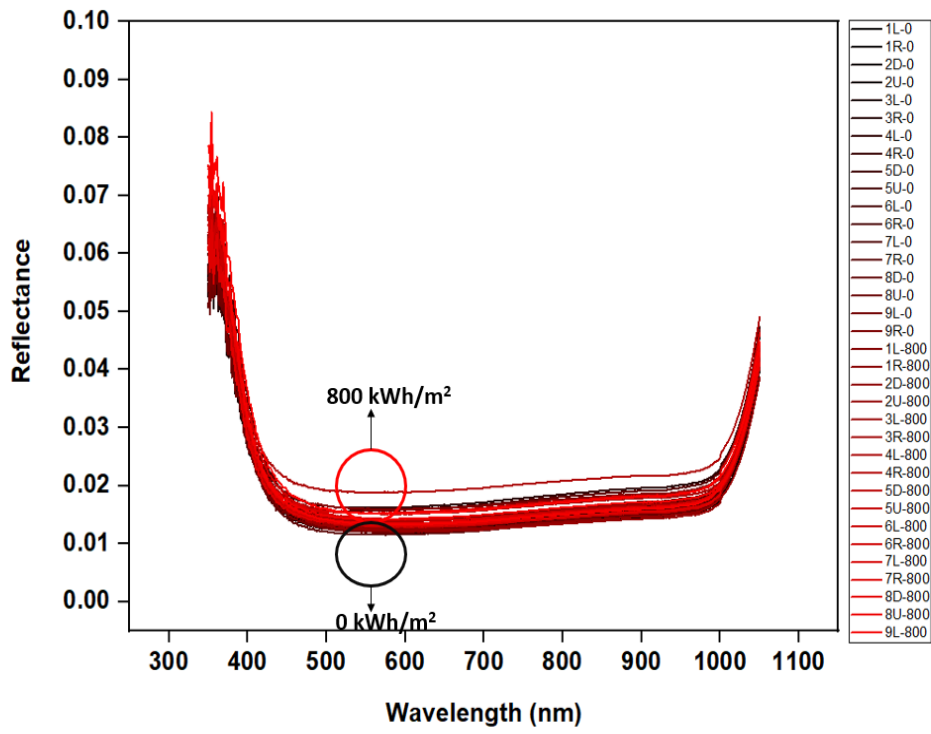
Figure 4.24:a) Reflectance plot for all cells in UVP-2 (dry run)
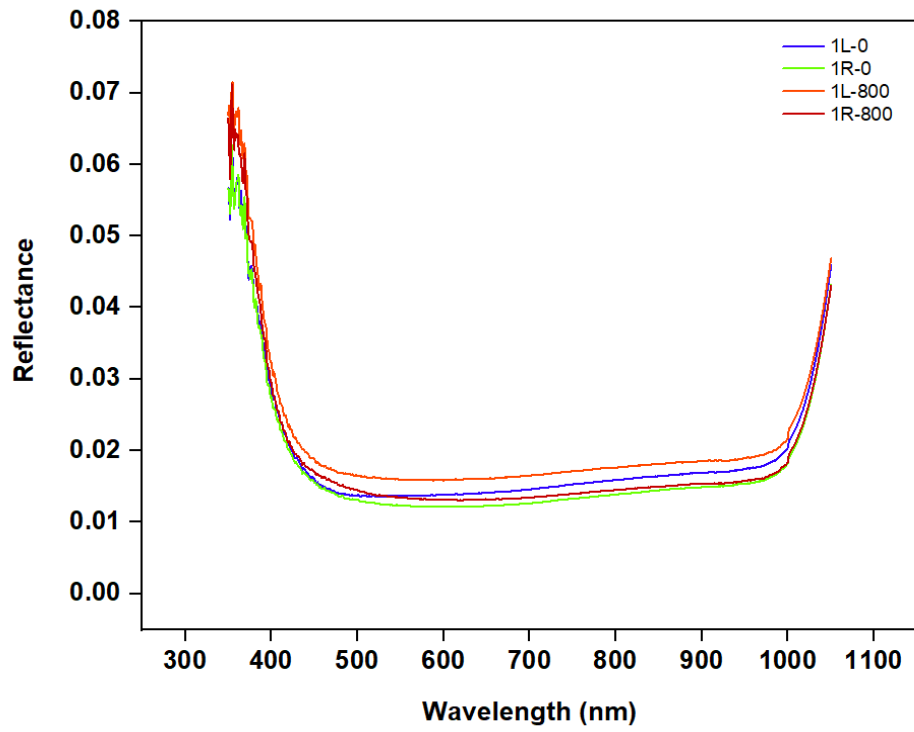
Figure 4.25:Reflectance for cell 1 at positions L and R of UVP-2 at 0 kWh/m^2 and 800 kWh/m^2
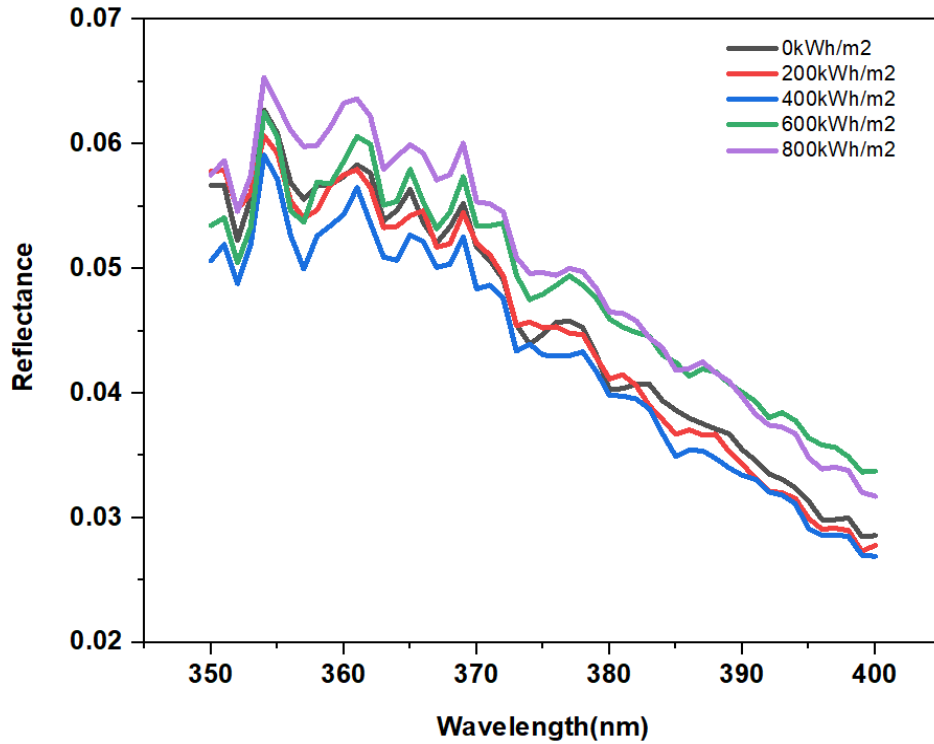
Figure 4.26: Reflectance study at 350 nm to 400 nm of the UVP coupons at 1L

At wavelength 350 – 400 nm, with higher dosage the reflectance is higher which is due to the lack of UV absorbers and hence the reflection is higher unlike in the case of the UV cut modules in the same wavelength range.

Figure 4.27 shows the reflectance of the UV cut module exposed to UV, temperature and humidity. The modules at 200 kWh/m²showed a higher reflectance than the modules which were unexposed before the test as shown in *Figure 4.27*.
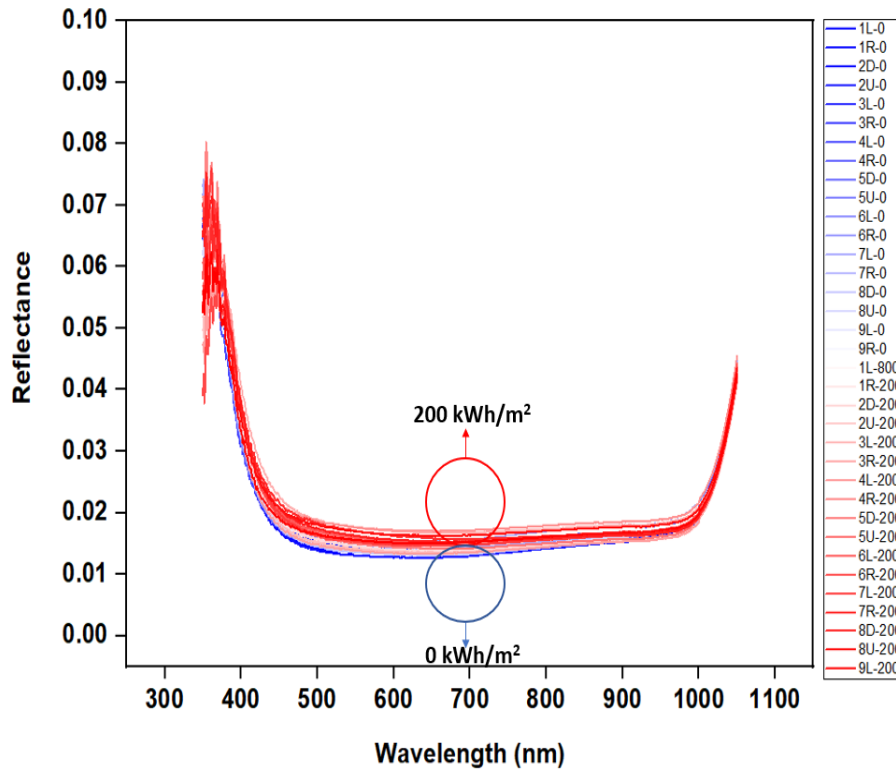
Figure 4.27: Reflectance plot for all cells for UV-Cut 0 kWh/m² and 200 kWh/m² (with humidity and oxygen)
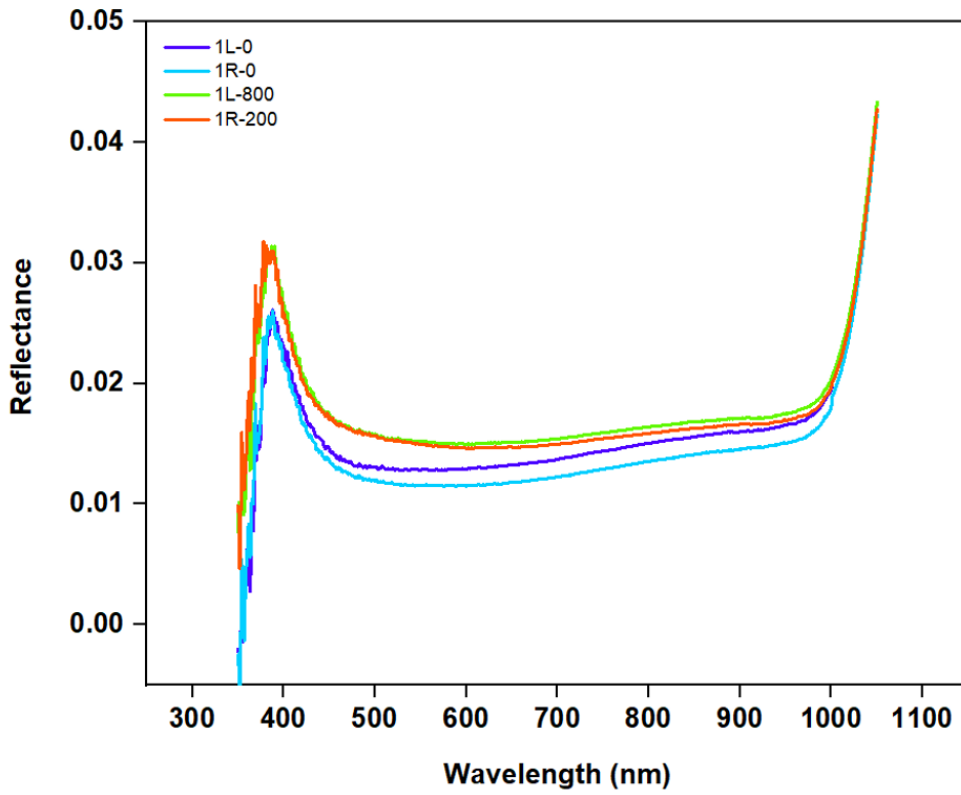
Figure 4.28:Reflectance for cell 1 at positions L and R of at 0 kWh/m^2 and 200 kWh/m^{2}of

high T humid cut module
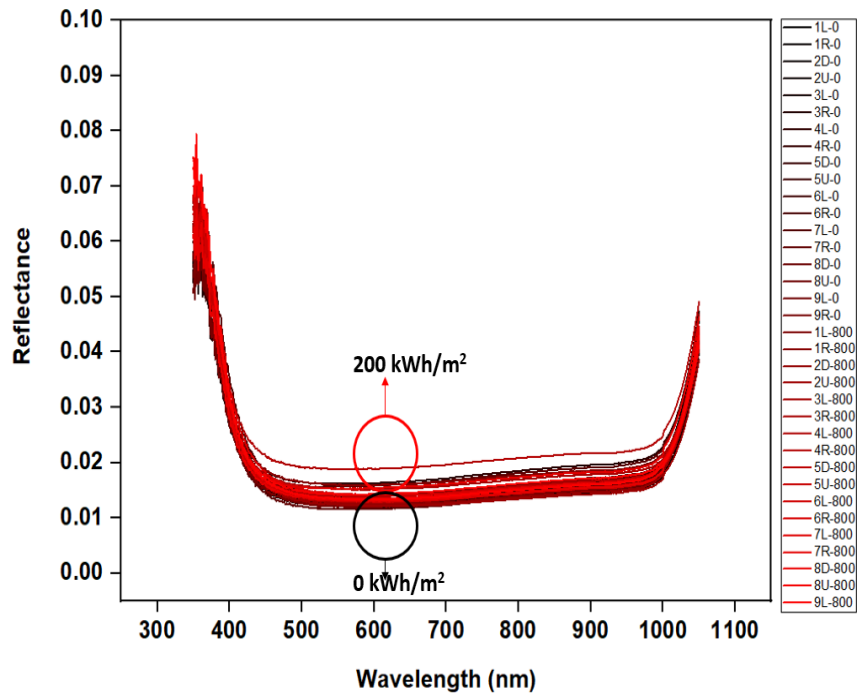
Figure4.29 : Reflectance plot for all cells in UV-Hybrid modules at 0 kWh/m^2 and 200 kWh/m^2 (with humidity and oxygen)
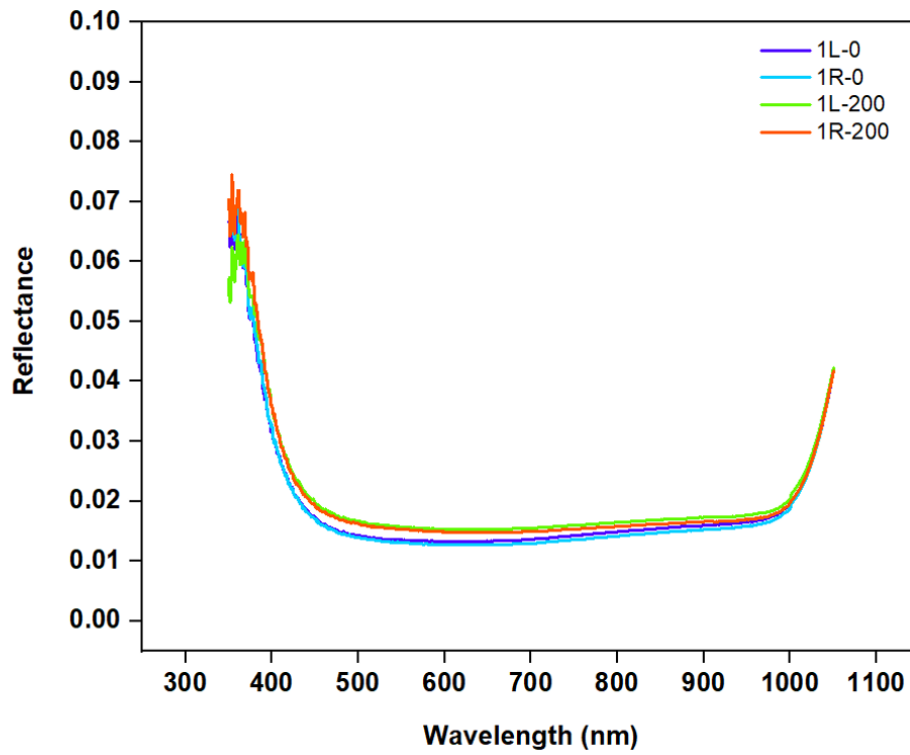
Figure 4.30:Reflectance for cell 1 at positions L and R of low T UVH at 0 kWh/m^{2}and 200 kWh/m^2

4.5 Correlation between Iscand YI

Figure 4.31 shows the Isc vs YI plot for UVC and UVP modules at various stages for the modules in the dry run. In UVC the median Isc decreases with an increase in the value of YI. This is a clear indication that the decrease in short circuit current is because of the discoloration observed. In the UV Pass modules, the change in YI is minimal. This shows that the drop in the short circuit current is due to delamination.
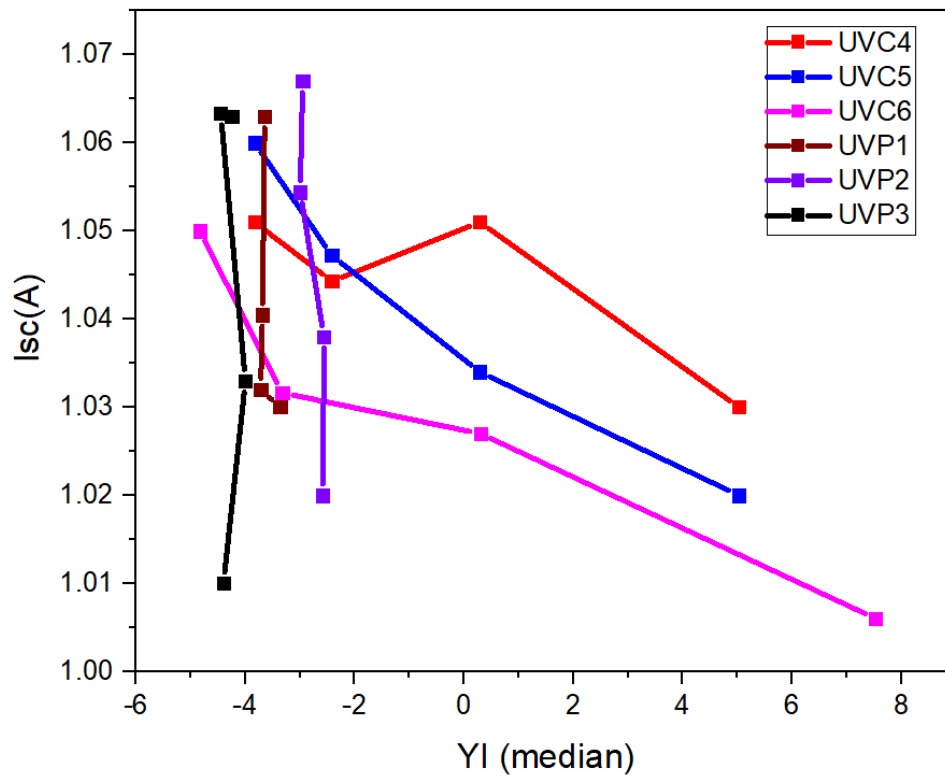
Figure 4.31: Isc vs YI plot for UVC and UVP modules at various stages of the dry accelerated stress test

For the humid run in *Figure 4.32*the values of the short circuit current decreases with an increase in the value of the YI. This indicates that the change in the material property of the EVA (loss in the transmission capacity due to discoloration) is the reason for the degradation in the short circuit current. In *Figure 4.32* the points in the top are at 0 kWh/m^{2}and points in the bottom are after 186 kWh/m^2.
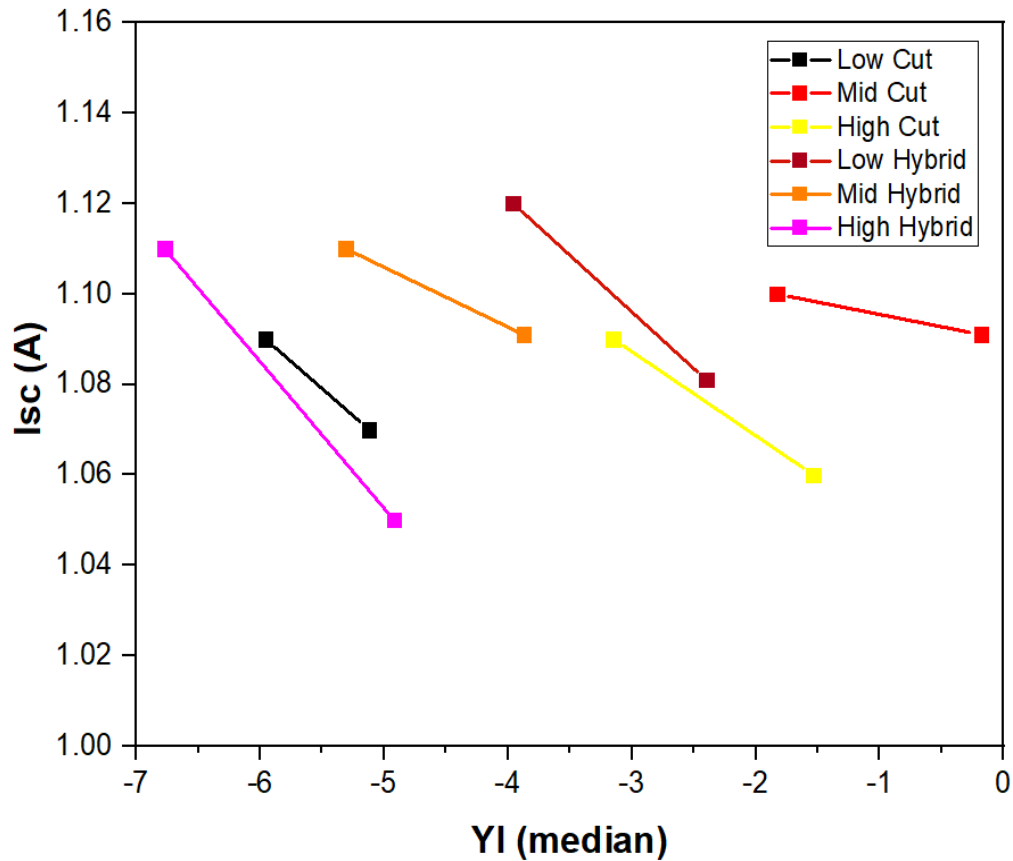
Figure 4.32:Isc vs YI plot for UVP modules at various stages of the humid accelerated stress test

Moreover, a good linear relationship can be obtained if the Isc is measured only in the browned region. In the above shown graphs the Isc is measured for the entire cell which includes both the browned area and the bleached area along the periphery.

4.6 Activation energy calculation

For the dry run at dosage of $400kWh/m^2$, $600kWh/m^2$ and $800kWh/m^2$ the activation energy is calculated by plotting 1/T vs ln (YI degradation rate). For this the YI degradation rate of all the cells at the two positions in the busbar are taken. Linear fit is done using origin and the parameters of regression coefficient is obtained. From the results the activation energy at 400 kWh/m^2 and 600 kWh/m^2 is 0.6 eVand $E_a$at 800 kWh/m^2 is 0.5 eV. At $800kWh/m^2$ there is a drop in the activation energy showing that there might be an additional mechanism in addition to discoloration which is occurring at 800 kWh/m^{2}dosage.
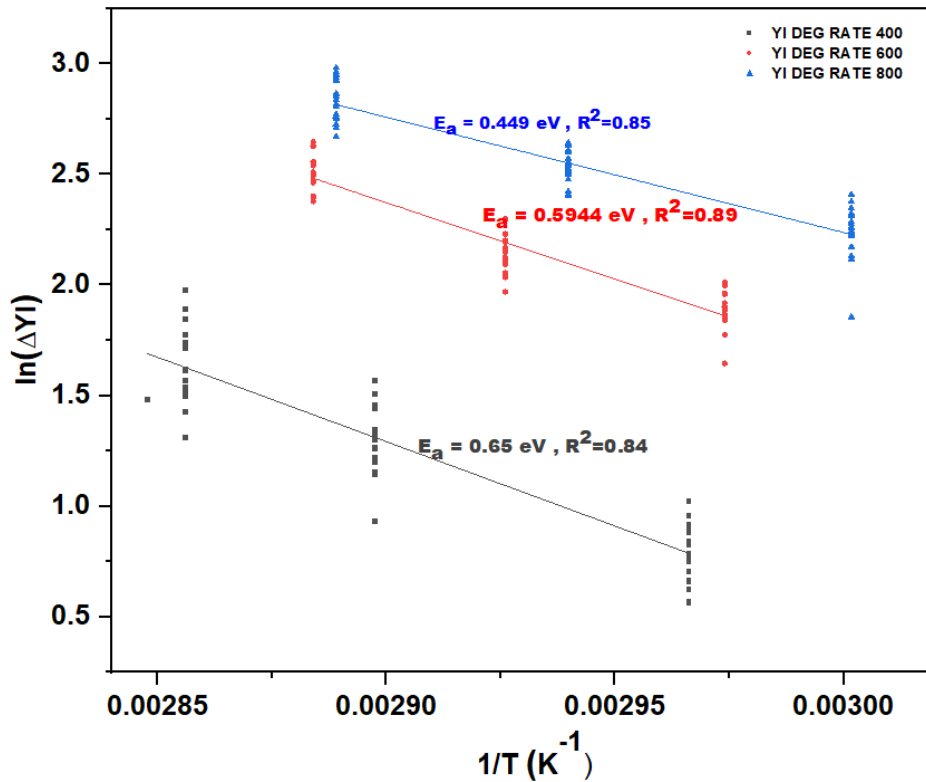
Figure 4.33: Activation energy with YI degradation rate at three different UV dosage each dosage having three different temperatures

By the mechanism suspected in*Pg29*, there is a possibility of the oxygen diffusing through the edges of the laminate. Hence the activation energy of all the cells will not give an accurate representation of the E_a for browning. To eliminate the possible bleaching effects and calculate the activation energy due to only browning, the corner cells are eliminated. The three cells in the center are considered for calculating the activation energy.
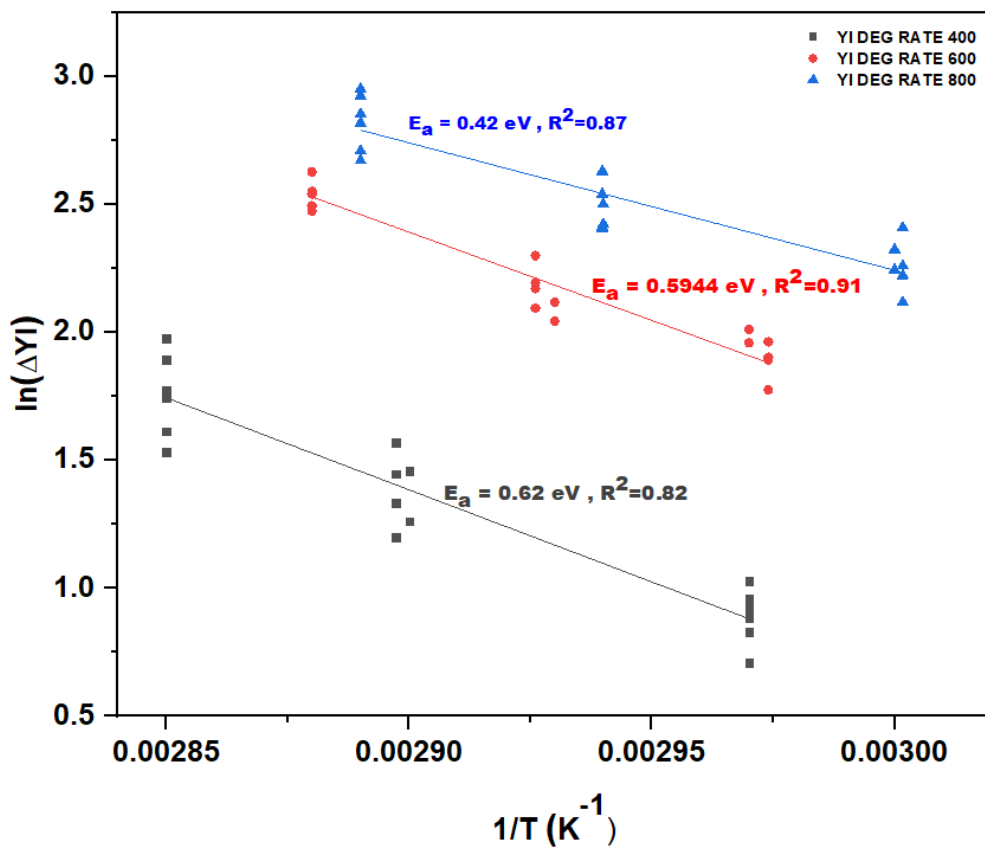
Figure 4.34:Activation energy with YI degradation rate at three different UV dosage each dosage having three different temperatures for the center cells (Cells 2,5,8)

5   CONCLUSIONS
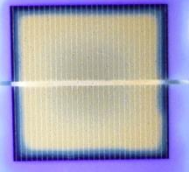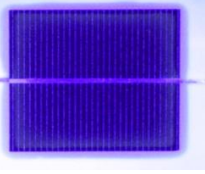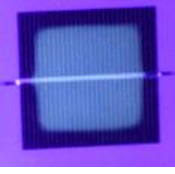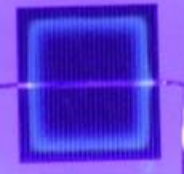
A walk-in UV chamber was used to investigate the durability and reliability issues of EVA encapsulant in PV modules. The UVC (both front and back of cells), UVP (both front and back of cells) and UVH (UVP front and UVC back of cells) EVA encapsulants were investigated in this study.

➢ In the UV-T-H testing of UVH modules, UVP encapsulant in the front side of the cell was not found to be discolored at the cell-center and cell-edge but was found to be discolored between the cell-center and cell-edge forming a discolored ring.With lack of UV absorbers, the discolored ring in the UVP appears to be formed due to two competing reactions: discoloration/hydrolysis of some of the additives due to the presence of humidity (lower molecular weight and faster diffusion rate) through the backsheetand bleaching due to the presence of oxygen (higher molecular weight and slower diffusion rate) through the backsheet.

➢ In the UV-T-H testing of UVC modules, the EVA discoloration was observed at the cell center as expected due to two competing reaction: discoloration of UV absorbing additives on the entire cell surface and bleaching of discolored UV absorbing additives at the cell edges due to the presence of oxygen at the cell edges.

➢ In the UV-T (dry run) testing of the UVC modules with aluminum tape on the backsheet, the browning/discoloration was expected throughout the cell surface due to the anticipated absence of oxygen at the cell edges. However, the browning

was observed only at the cell center with no browning at the cell edges. This indicated the presence of oxygen at the cell edges. The presence of oxygen at the cell edges is attributed to the failure of aluminum tape's adhesive during the prolonged test. Due to this adhesion failure of aluminum tape, it seems oxygen ingresses from the laminate edges to the cell edges through the interface between backsheet and aluminum tape.

➢ In the UV-T (dry run) testing of the UVP modules with aluminum tape on the backsheet, no browning/discoloration was expected due to the absence of UV absorbing additives. However, it seems that the UVP encapsulant suffers from a delamination issue without any discoloration issue.

➢ The UV fluorescence images of UV-T (dry run) and UV-T-H (humid run) modules are summarized in Table 5.1

71

Table 5.1: UVF images of discolored and delaminated EVA encapsulant

Dry Run (UVC with Al) @ 800 kWh/m²	Dry Run (UVP with Al) @ 800 kWh/m²	Humid Run (UVC w/o Al) @ 200 kWh/m²	Humid Run (UVH w/o Al) @ 200 kWh/m²
Discoloration at cell center with slight edge bleaching	Delamination over cell surface and edges	Discolored center	Discolored ring formation

> The activation energy determined in the UV-T testing of PV modules are summarized in Table 5.2

Table 5.2: Activation energy of EVA browning determined for the UV-T (dry run) modules using yellowness index method

Dry Run	All nine cells	E_a @ 400 kWh/m^2 (eV)	E_a @ 600 kWh/m^2 (eV)	E_a @ 800 kWh/m^2 (eV)
		0.6523	0.596	0.4494
	Center cells (Cells 2, 5, 8)	0.6236	0.5944	0.424

A decrease in activation energy was observed when the UV dosage was increased from 600 kWh/m^2 to 800 kWh/m2. The reason for this decrease in activation energy is unknown but it could be due to the induction of an additional reaction along with the browning reaction.

REFERENCES

[1]   X. L., T. P. Prawiradiraja, and . D. B., "The Role of Humidity in Energy Output of Solar Panels in Coastal Regions," *GSTF J. Eng. Technol.*, vol. 2, no. 1, 2014.

[2]   C. Peike, I. Hadrich, K. Weiß, I. Durr, and F. Ise, "Overview of PV module encapsulation materials," *Pvi*, vol. 22, no. November 2015, pp. 85–92, 2013.

[3]   D. Wu, J. Zhu, T. R. Betts, and R. Gottschalg, "PV module degradation mechanisms under different environmental stress factors," in *8th Photovoltaic Science Application and Technology Conference (PVSAT-8)*, 2012.

[4]   M. C. C. de Oliveira, A. S. A. Diniz Cardoso, M. M. Viana, and V. de F. C. Lins, "The causes and effects of degradation of encapsulant ethylene vinyl acetate copolymer (EVA) in crystalline silicon photovoltaic modules: A review," *Renewable and Sustainable Energy Reviews*. 2018.

[5]   M. Kumar Panjwani and G. Bukshsh Narejo, "Effect of Humidity on the Efficiency of Solar Cell (photovoltaic)," *Int. J. Eng. Res. Gen. Sci.*, vol. 2, no. 4, 2014.

[6]   E.M, "Difference between humidity and relative humidity," *DifferenceBetween.net*, 2017.

[7]   J. H. Wohlgemuth and S. Kurtz, "Using accelerated testing to predict module reliability," in *Conference Record of the IEEE Photovoltaic Specialists Conference*, 2011.

[8]   F. Pern J., "EVA Encapsulants for PV: Degradation and Discoloration Mechanisms and Formulation Modifications for Improved Photostability," *Die Angew. Makromol. Chemie*, 1997.

[9]   F. J. Pern and A. W. Czanderna, "EVA degradation mechanisms simulating those in PV modules," in *AIP Conference Proceedings*, vol. 268, pp. 445–452,1992.

[10]   P. Klemchuk, M. Ezrin, G. Lavigne, W. Holley, J. Galica, and S. Agro, "Investigation of the degradation and stabilization of EVA-based encapsulant in field-aged solar energy modules," *Polym. Degrad. Stab.*, vol. 55, no. 3, pp. 347–365, 1997.

[11]   C. Ballif *et al.*, "Impact of moisture ingress in PV modules on long-term performance: the role of EVA formulation, module design and climate," 2014.

[12]   U. Weber *et al.*, "Acetic acid production, migration and corrosion effects in ethylene-vinyl-acetate-(EVA-) based PV modules," *PVSEC 27th*, vol. 27. pp. 2992–2995, 2012.

[13]   J. Zhu, D. Montiel-Chicharro, T. Betts, and R. Gottschalg, "Correlation of degree

of EVA crosslinking with formation and discharge of acetic acid in PV modules," in *33rd European Photovoltaic Solar Energy Conference and Exhibition (PVSEC 2017)*, pp. 1795–1798, 2017.

[14]   E. Wang, H. E. Yang, J. Yen, S. Chi, and C. Wang, "Failure modes evaluation of PV module via materials degradation approach," in *Energy Procedia*, 2013.

[15]   M. Köntges *et al.*, "Assessment of Photovoltaic Module Failures in the Field," *IEA Photovoltaic Power Systems*. pp. 1–73, 2017.

[16]   K. Eder, Gabriele & voronko, yuliya & grillberger, paul & kubicek, bernhard & Knöbl, "UV-Fluorescence measurements as tool for the detection of degradation effects in PV- Modules," in *8th European Weathering Symposium; Natural and Artificial Ageing of Polymers*, 2017.

[17]   A. Badiee, "An examination of the response of ethylene-vinyl acetate film to changes in environmental conditions," 2016.

[18]   D. J. V. Kumar, "Determination of Activation Energy for Encapsulant Browning of Photovoltaic Modules," Masters Thesis, Arizona State University, 2016.

[19]   K. Dolia, "Accelerated UV Testing and Characterization of PV Modules with UV-cut and UV-pass EVA Encapsulants," Arizona State University, 2018.

[20]   G. C. Eder, Y. Voronko, C. Hirschl, R. Ebner, G. Újvári, and W. Mühleisen, "Non-destructive failure detection and visualization of artificially and naturally aged PV modules," *Energies*, 2018.

[21]   M. S. A. Morlier, M. Köntges and I. Kunze, "UV fluorescence imaging as fast inspection method for PV modules in the field," in *14th IEA PVPS Task 13 Meeting Bolzano*, 2016.

[22]   K. K. Mokwena and J. Tang, "Ethylene Vinyl Alcohol: A Review of Barrier Properties for Packaging Shelf Stable Foods," *Critical Reviews in Food Science and Nutrition*. 2012.

[23]   J. B. R. William B. Hobbs, Braden Gilleland, "Fast acquisition of UV-Fluorescence images and automated crack detection," 2019.

[24]   J. Lin, "UVFL Inspection: Drones and Tools,"*PV Guide*r, 2018.

[25]   N. C. Park, J. S. Jeong, B. J. Kang, and D. H. Kim, "The effect of encapsulant discoloration and delamination on the electrical characteristics of photovoltaic module," in *Microelectronics Reliability*, 2013.